1   # Antibody Evolution after SARS-CoV-2 mRNA Vaccination

2

3   Alice Cho[1,*], Frauke Muecksch[2,*], Dennis Schaefer-Babajew[1,*], Zijun Wang[1,*], Shlomo

4   Finkin[1,*],Christian Gaebler[1], Victor Ramos[1], Melissa Cipolla[1], Marianna Agudelo[1], Eva

5   Bednarski[2], Justin DaSilva[2], Irina Shimeliovich[1], Juan Dizon[1], Mridushi Daga[1], Katrina Millard[1],

6   Martina Turroja[1], Fabian Schmidt[2], Fengwen Zhang[2], Tarek Ben Tanfous[1], Mila Jankovic[1],

7   Thiago Y. Oliveria[1], Anna Gazumyan[1], Marina Caskey[1], Paul D. Bieniasz[2,3], Theodora

8   Hatziioannou[2], and Michel C. Nussenzweig[1,3].

9

10   [1]Laboratory of Molecular Immunology, The Rockefeller University, New York, NY 10065, USA

11   [2]Laboratory of Retrovirology, The Rockefeller University, New York, NY 10065, USA

12   [3]Howard Hughes Medical Institute

13

14   *equal contribution

15   Address correspondence to: Paul D. Bieniasz pbieniasz@rockefeller.edu; Marina Caskey
16   mcaskey@rockefeller.edu; Theodora Hatziioannou thatziio@rockefeller.edu; or Michel C.
17   Nussenzweig nussen@rockefeller.edu
18

19   **Summary**

20   **Severe acute respiratory syndrome coronavirus 2 (SARS-CoV-2) infection produces B-cell**

21   **responses that continue to evolve for at least one year. During that time, memory B cells**

22   **express increasingly broad and potent antibodies that are resistant to mutations found in**

23   **variants of concern[1]. As a result, vaccination of coronavirus disease 2019 (COVID-19)**

24   **convalescent individuals with currently available mRNA vaccines produces high levels of**

25   **plasma neutralizing activity against all variants tested[1,2]. Here, we examine memory B cell**

26   **evolution 5 months after vaccination with either Moderna (mRNA-1273) or Pfizer-**

27   **BioNTech (BNT162b2) mRNA vaccines in a cohort of SARS-CoV-2 naïve individuals.**

28   **Between prime and boost, memory B cells produce antibodies that evolve increased**

29   **neutralizing activity, but there is no further increase in potency or breadth thereafter.**

30   **Instead, memory B cells that emerge 5 months after vaccination of naïve individuals**

31   **express antibodies that are equivalent to those that dominate the initial response. We**

32   **conclude that memory antibodies selected over time by natural infection have greater**

33   **potency and breadth than antibodies elicited by vaccination. These results suggest that**

34   **boosting vaccinated individuals with currently available mRNA vaccines would produce a**

35   **quantitative increase in plasma neutralizing activity but not the qualitative advantage**

36   **against variants obtained by vaccinating convalescent individuals.**

37

38   Between January 21 and June 23, 2021, we recruited 32 volunteers with no history of prior

39   SARS-CoV-2 infection receiving either Moderna (mRNA-1273; n=8) or Pfizer-BioNTech

40   (BNT162b2; n=24) mRNA vaccines for sequential blood donation. Matched samples were

41   obtained an average of 2.5 and 5 weeks after the prime and boost, respectively, and an additional

2

42   set of matched samples an average of 2 and 5 months after the boost. The volunteers ranged in

43   age from 23-78 years (median 34.5 years), 53% were male and 47% female (for details see

44   Methods and Supplementary Tables 1 and 2).

45

46   **Plasma binding and neutralization assays**

47   Plasma IgM, IgG, and IgA responses to SARS-CoV-2 receptor binding domain (RBD) were

48   measured by enzyme linked immunosorbent assay (ELISA)[3]. As reported by others[2,4-6] there was

49   a significant increase in IgG reactivity to RBD between prime and boost (p<0.0001, Fig. 1a).

50   IgM and IgA titers were lower than IgG titers and remained low after the second vaccine dose

51   (Extended data Fig. 1a and b). The magnitude of the response was inversely correlated with age

52   after the prime (r=-0.54, p=0.005), but the difference was no longer significant after the boost

53   (Fig. 1b). Between 2 and 5 months after the boost, anti-RBD titers of all isotypes decreased

54   significantly. IgG titers decreased by an average of 5.2-fold (range: 2.1- to 10.2-fold) and the

55   loss of activity was directly correlated to the time after vaccination (p<0.0001, Fig. 1c and d and

56   Extended data Fig. 1c and d).

57

58   Neutralizing activity was measured using HIV-1 pseudotyped with the SARS-CoV-2 spike[1,3,7,8].

59   Naïve individuals showed variable responses to the initial vaccine dose with a geometric mean

60   half-maximal neutralizing titer (NT_{50}) of 171 (Fig. 1e and Supplementary Table 2). The

61   magnitude of the neutralizing responses to the initial vaccine dose in naïve volunteers was

62   inversely correlated with age (r=-0.39, p=0.05, Fig. 1f). Both binding and neutralizing responses

63   to the second vaccine dose were correlated to the prime (r=0.46, p=0.02, Extended data. Fig. 1e;

64   r=0.54, p=0.003, Extended data Fig. 1f) and produced a nearly 15-fold increase in the geometric

3

65   mean neutralizing response that was similar in males and females and eliminated the age-related

66   difference in neutralizing activity (Extended data 2g and Fig. 1f). After the boost naïve vaccinees

67   had 6.2-fold higher neutralizing titers than a cohort of infected individuals measured 1.3 months

68   after symptom onset[3] (p<0.0001, Fig. 1e). Neutralizing responses were directly correlated to IgG

69   anti-RBD titers (r=0.96, p<0.0001, Fig. 1g). Thus, the data obtained from this cohort agree with

70   prior observations showing a significant increase in plasma neutralizing activity that are

71   correlated with improved vaccine efficacy in naïve individuals that receive the second dose of

72   mRNA vaccine[2,6,9,10].

73

74   The 15 individuals assayed 5 months after vaccination had an average 4.7-fold decrease in

75   geometric mean neutralizing activity from their 2-month measurement (p=0.04, Fig. 1h), with a

76   range of 1.4- to 27-fold (Fig. 1i). Neutralizing activity was inversely correlated with the time

77   from vaccination (r=-0.75, p<0.0001, Fig. 1j), and directly correlated to IgG anti-RBD binding

78   titers when assessed 5 months after vaccination (Extended data. Fig. 1h).

79

80   We and others showed that the neutralizing responses elicited by mRNA vaccination are more

81   potent against the original Wuhan Hu-1 strain than for some of the currently circulating variants

82   of concern[2,11-13]. To confirm these observations, we measured the neutralizing activity of the

83   paired plasmas from naive individuals 2 and 5 months after the second vaccine dose against

84   B.1.1.7 (alpha variant), B.1.351 (beta variant), B.1.526 (first isolated in New York City), P.1

85   (gamma variant) and B.1.617.2 (delta variant). Consistent with previous reports[12,14-16] the

86   neutralizing activity against the variants was lower than against the original Wuhan Hu-1 strain

87   (Fig. 1k, Supplementary Table 3). Initial geometric mean neutralizing titers at 2 months against

88   B.1.351, B.1.1.7, B.1.526, P.1 and B.1.617.2 were 5.7, 1.8, 1.1, 1.4 and 2.7-fold lower than

89   against Wuhan-Hu respectively (Fig. 1k). In the months following vaccination there was a

90   decrease in neutralizing activity against all variants that paralleled the drop in activity against

91   Wuhan Hu-1 (R683G) with geometric mean neutralizing titers for WT, B.1.351, B.1.1.7,

92   B.1.526, P.1 and B.1.617.2 decreasing by 2.9-, 1.8-, 2.3-, 2.9-, 2.4- and 2.6-fold, respectively

93   (Fig. 1k and Supplementary Table 3). Nevertheless, vaccine-induced neutralizing activity at 5

94   months against all variants exceeds Wuhan-Hu plasma neutralization of convalescent individuals

95   after 6.2 months.

96

97

98   **Monoclonal Antibodies**

99   Circulating antibodies produced by plasma cells can prevent infection if present at sufficiently

100   high concentrations at the time of exposure. In contrast, the memory B cell compartment

101   contains long lived antigen-specific B cells that mediate rapid recall responses that contribute to

102   long term protection[17]. To examine the nature of the memory compartment elicited by one or two

103   mRNA vaccine doses and its evolution after 5 months we used flow cytometry to enumerate B

104   cells expressing receptors that bind to Wuhan Hu-1 (wild type) and the B.1.351

105   K417N/E484K/N501Y (KEN) variant RBDs (Fig. 2a and b, and Extended data Fig. 2). Wuhan-

106   Hu RBD-specific memory B cells developed after the prime in all volunteers examined and their

107   numbers increased for up to 5 months after vaccination (Fig. 2a). Memory B cells binding to the

108   B.1.351 RBD were detectable but in lower numbers than wild type RBD-binding B cells in all

109   samples examined (Fig. 2b). Whereas IgG memory cells increased after the boost, IgM-

110   expressing memory B cells that made up 23% of the memory compartment after the prime were

111   nearly absent after boosting (Fig. 2c). Finally, circulating RBD-specific plasmablasts were

112   readily detected after the prime but were infrequent after the boost (Fig. 2d, and Extended data

113   Fig. 2d).

114

115   The memory compartment continues to evolve up to one year after natural infection with

116   selective enrichment of cells producing broad and potent neutralizing antibodies[1]. To determine

117   how the memory compartment evolves after vaccination, we obtained 1524 paired antibody

118   sequences from 6 individuals sampled at 2.5 weeks after prime and 5 weeks or 5 months after

119   boost, and an additional 804 paired antibody sequences from 5 individuals sampled after 2- or 5-

120   months after boost (Fig. 2e and f, Extended Data Fig 3, Supplementary Table 4). As expected

121   *IGHV3-30* and *IGHV3-53* were over-represented after the first and second vaccine dose and

122   remained over-represented 5 months after vaccination[18-20] (Extended data Fig. 4).

123

124   All individuals examined showed expanded clones of memory B cells that expressed closely

125   related IGHV and IGHL genes (Fig. 2e and f, Extended data Fig. 4). Paired prime and boost

126   samples showed expanded clones of memory B cells some of which were shared across

127   plasmablast, IgM and IgG prime, and IgG boost memory cells (Extended data Fig. 3 and 5).

128   Thus, the cell fate decision controlling the germinal center versus plasmablast decision is not

129   entirely affinity dependent since cells with the same initial affinity can enter both

130   compartments[21].

131

132   The relative fraction of memory cells found in expanded clones varied between prime and boost

133   and between individuals (Fig. 2e). However, new clones that develop after the boost represent a

134   greater fraction (80%) of the total clones than the conserved clones in all individuals (Fig. 2e).

135   Finally, memory B cells emerging after the boost showed significantly higher levels of somatic

136   mutations than plasmablasts or memory B cells isolated after the prime (Extended data Fig. 3b).

137

138   After 5 months, there was an overall decrease in the percentage of clones in the RBD-binding

139   memory compartment (Fig. 2g). Nevertheless, clones of memory B cells continued to evolve for

140   up to 5 months in vaccinated individuals as evidenced by the dominance of newly emerging

141   clones (86%, Fig. 2e and f) and the significant increase in somatic mutation between the time

142   points (p<0.0001, Fig. 2h, Extended data Fig. 3c). The number of mutations in antibody genes

143   was comparable between vaccinated and convalescent individuals after 5 months (Fig. 2h,

144   Extended data Fig. 3c). In conclusion the memory B cell compartment continues to evolve for up

145   to 5 months after mRNA vaccination.

146

147   **Neutralizing Activity of Monoclonal Antibodies**

148   We performed ELISAs to confirm that the antibodies isolated from memory B cells bind to RBD

149   (Extended data Fig. 6). 403 antibodies were tested by ELISA including: 86 isolated after the first

150   vaccine dose; 92 isolated after the second vaccine dose; 111 isolated 2 months after the second

151   vaccine dose and 114 isolated from individuals that had been fully vaccinated 5 months earlier.

152   Among the 403 antibodies tested 381 (95%) bound to the Wuhan Hu-1 RBD indicating that the

153   method used to isolate RBD-specific memory B cells was highly efficient (Supplementary Table

154   5-7). The geometric mean ELISA half-maximal concentration (EC_{50}) of the antibodies obtained

155   after prime, boost, 2 months and 5 months was 3.9, 2.6, 3.2 and 2.8 ng/ml respectively,

156   suggestive of no change in binding over time after vaccination (Extended data Fig. 6 and

157 Supplementary Table 5). Binding among all antibodies did not improve between prime and

158 boost, or 2 and 5 months (Extended data Fig. 6). However, a slight improvement was observed

159 after 5 months among clones (Extended data Fig.6).

160

161 381 RBD-binding antibodies were tested for neutralizing activity using HIV-1 pseudotyped with

162 the SARS-CoV-2 spike[3,8]. The geometric mean half-maximal inhibitory concentration (IC_{50}) of

163 the RBD-specific memory antibodies improved from 380 ng/ml to 170 ng/ml between the first

164 and second vaccine dose (p=0.005, Fig. 3a). The improvement was reflected in all clones (IC_{50}

165 370 vs. 182 ng/ml, p=0.03 Fig. 3b), newly arising clones (IC_{50} 430 vs. 165 ng/ml, p=0.02 Fig.

166 3c), single antibodies (IC_{50} 357 vs. 131 ng/ml, Fig. 3d) and conserved clones (IC_{50} 314 vs. 208

167 ng/ml, Fig. 3e, Supplementary Table 6). The increase in neutralizing activity between the first

168 and second vaccine dose was associated with a decrease in the percentage of non-neutralizing

169 antibodies (defined as IC50 >1000ng/ml) and increased representation of neutralizing antibodies

170 (p= 0.03, Fig. 3a). In conclusion, memory B cells recruited after the boost account for most of

171 the improvement in neutralizing activity in this compartment between the 2 vaccine doses. Thus,

172 in addition to the quantitative improvement in serum neutralizing activity there is a qualitative

173 improvement in the memory compartment after boosting.

174

175 There was no further improvement in neutralizing activity of the monoclonal antibodies obtained

176 between 2 and 5 months after vaccination (IC_{50} 140 vs. 144 ng/ml, Fig. 3f). This was true when

177 considering all B cell clones, newly arising clones or single memory B cells separately (Fig. 3g-j,

178 Supplementary table 7). In contrast, memory antibodies obtained from convalescent individuals

179 showed improved neutralizing activity between 1.3[3] and 6.2 months[7] with IC_{50} of 171 ng/ml to

180   116 ng/ml (Fig. 3f), which improved further after 1 year[1]. This improvement was due to

181   increased neutralizing activity among persisting clones (p=0.003, Fig. 3h).

182

183   **Affinity, Epitopes and Neutralization Breadth**

184   To examine affinity maturation after vaccination, we performed biolayer interferometry (BLI)

185   experiments using the Wuhan Hu-1 RBD[3]. 60 randomly selected antibodies were assayed from

186   the prime-boost cohort, 30 obtained after the prime and 30 after the boost, with similar overall

187   geometric mean IC_{50}s ranging from <10 ng/ml to >1000 ng/ml (Extended data Fig. 7a). There

188   was no significant difference in affinity between the antibodies obtained after the prime and

189   boost, and no correlation between affinity and neutralizing activity (Fig. 4a and Extended Data

190   Fig. 7 b and c). Similar experiments were performed on 31 and 30 antibodies obtained from the

191   2- and 5-month time points from vaccinated individuals, respectively. Despite similar levels of

192   neutralizing activity (Extended data Fig. 7d), there was an average 2.6-fold increase in the

193   affinity of the antibodies obtained between 2 and 5 months after vaccination (p=0.02, Fig. 4b and

194   Extended Data Fig. 7e and f).

195

196   We also compared the affinities of pairs of antibodies obtained from conserved clones between 2

197   and 5 months after vaccination. Conserved clones obtained at 2 and 5 months from vaccinated

198   individuals showed an average 1.9-fold increase in affinity (p=0.03, Fig. 4c). In contrast, a

199   comparable group of conserved clonal antibodies obtained from convalescent individuals 1.3 and

200   6.2 months after infection showed an average 24-fold increase in affinity (p=0.002, Fig. 4c).

201

202   In addition to the increase in potency, the neutralizing breath of memory antibodies obtained

203   from conserved clones from convalescent individuals increases with time after infection[1,7,22]. To

204   determine whether there is a similar increase in breadth with time after vaccination, we selected

205   20 random antibodies from the prime or boost, with representative levels of activity against the

206   original Wuhan Hu-1 strain, and measured their neutralization potency against a panel of

207   psudotypes encoding RBD mutations associated with circulating variants of concern (Extended

208   data. Fig. 8). There was little change in breadth between prime and boost, with only a small

209   increase in resilience to K417N and A475V substitutions (Extended data Fig. 8, Supplementary

210   Table 8).

211

212   In addition, we assayed 10 conserved pairs of neutralizing antibodies obtained 2 and 5 months

213   after vaccination against the same RBD mutant pseudotypes (Fig. 4d and Supplementary Table

214   9). They were compared to 6 previously reported[22], plus 10 additional pairs of antibodies

215   obtained from convalescent individuals at 1.3- and 6.2-month time points (Fig. 4e and

216   Supplementary Table 9). Whereas only 4 of 10 of the vaccine antibodies showed improved

217   breadth, 15 of the 16 convalescent pairs developed increased breadth. Moreover, only 1 of the 10

218   vaccine antibody pairs showed improved potency against pseudotypes carrying B.1.617.2 (delta

219   variant)-specific RBD amino acid substitutions (L452R/T478K), while 11 out of 16 convalescent

220   antibody pairs showed improved activity against this virus (Fig. 4d and e). We conclude that

221   antibody evolution differs in convalescent and vaccinated individuals in that there is less affinity

222   maturation and little increase in breadth between 2 and 5 months after mRNA vaccination.

223

224   Circulating antibodies are produced by plasma cells with variable longevity[23-26]. SARS-CoV-2

225   infection or mRNA vaccination produces an early peak antibody response that decreases by 5-

226   10-fold after 5 months[7,27-31]. Notably, peak neutralization titres after vaccination exceed those of

227   COVID-19 recovered individuals. Nevertheless, neutralizing potency against variants is

228   significantly lower than against Wuhan Hu-1, with up to 5-10-fold reduced activity against the

229   B.1.351 variant[5,6,12,13,32]. Taken together with the overall decay in neutralizing activity there can

230   be 1-2 orders of magnitude decrease in serum neutralizing activity after 5 or 6 months against

231   variants when compared to the peak of neutralizing activity against Wuhan Hu-1. Thus, antibody

232   mediated protection against variants is expected to wane significantly over a period of months,

233   consistent with reports of reinfections in convalescent individuals and breakthrough infection by

234   variants in fully vaccinated individuals[33-35].

235

236   In contrast to circulating antibodies, memory B cells are responsible for rapid recall responses[36-

237   39], and this compartment is relatively stable over the first 6 months after natural infection[7,40] or

238   mRNA vaccination. In both cases memory B cells continue to evolve for up to 5 months as

239   evidenced by increasing levels of somatic mutation and emergence of newly expanded clones.

240

241   The memory response would be expected to protect individuals that suffer breakthrough

242   infection from developing serious disease. However, memory B cell evolution differs in

243   important ways between infection and mRNA vaccination. Both natural infection and mRNA

244   vaccination produce memory antibodies that evolve increased affinity, but the increase in affinity

245   is more modest after vaccination. This difference is consistent with the observation that vaccine-

11

246   elicited memory antibodies fail to show the increased neutralizing breadth that developed after

247   natural infection[1,7].

248

249   There are innumerable differences between natural infection and mRNA vaccination that could

250   account for the differences in antibody evolution over time. These include but are not limited to:

251   1. Route of antigen delivery, respiratory tract vs. intra-muscular injection[41,42]; 2. The physical

252   nature of the antigen, intact virus vs. S protein[43]; 3. Antigen persistence, weeks in the case of

253   natural infection[7] vs. hours to days for mRNA[44]. Each of these could impact on B cell evolution

254   and selection directly, and indirectly through differential T cell recruitment.

255

256   The increase in potency and breadth in the memory compartment that develops after natural

257   infection accounts for the exceptional responses to Wuhan Hu-1 and its variants that

258   convalescent individuals develop when boosted with mRNA vaccines[1,5]. The expanded memory

259   B cell compartment in mRNA vaccinees should also produce high titers of neutralizing

260   antibodies but with decreased breath in comparison to natural infection when vaccinees are

261   boosted or when they are re-exposed to the virus[45].Thus, boosting vaccinated individuals with

262   currently available mRNA vaccines will produce strong responses that mirror their initial vaccine

263   responses to Wuhan-Hu with similarly decreased coverage against variants. Finally, timing a

264   boost for optimal responses will depend on whether the objective is to prevent viral acquisition

265   or disease[46]. Given the rapid emergence of variants, in the former, boosting would be needed on

266   a far shorter time scale than the latter. The optimal timing for boosting to prevent serious disease

267   will depend on the stability and further evolution of the memory B cell compartment.

268

269   **FIGURES**

270
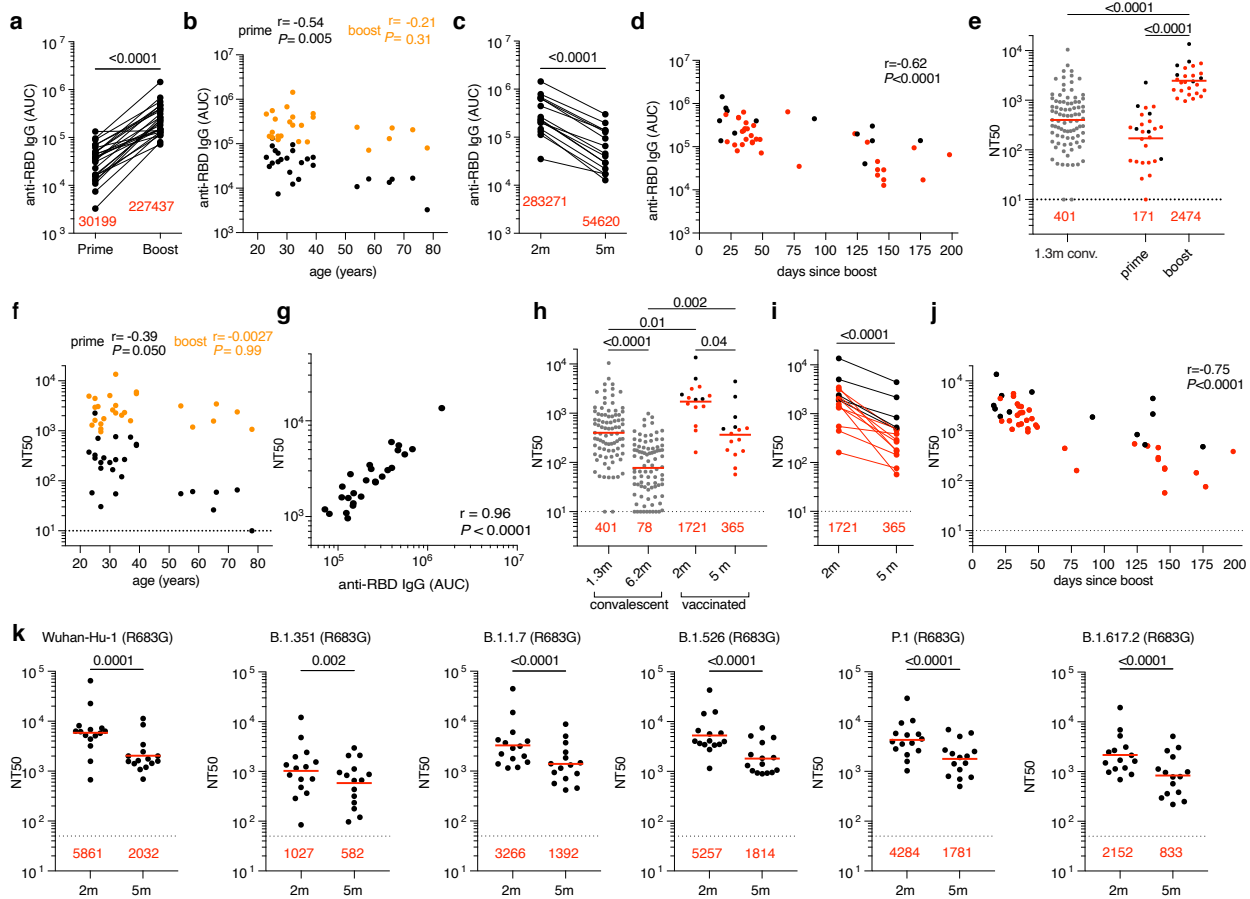
Fig. 1: Plasma ELISAs and neutralizing activity.

272   **a,** Graph shows area under the curve (AUC, Y-axis) for plasma IgG antibody binding to SARS-

273   CoV-2 RBD after prime and boost for paired samples. (n=26) **b,** Graph shows plasma IgG antibody

274   binding (AUC, Y-axis) plotted against age (X-axis) after prime (black) and boost (orange). **c,**

275   Graph shows AUC (Y-axis) for plasma IgG antibody binding to SARS-CoV-2 RBD for paired

276   samples obtained 2 and 5 months after the boost. (n=15) **d,** Graph shows AUC values from **a**, and

277   **b,** (Y-axis) plotted against time after vaccination (X-axis). **e,** NT50 in convalescent individuals

278   1.3m after infection[3] and in vaccinated individuals after 1 dose (prime) or 2 doses (boost) of an

279   mRNA vaccine. **f**, NT50 values (Y-axis) vs. age (years X-axis) in individuals receiving 1 dose

280   (prime, black) or two doses (boost, orange) of an mRNA vaccine. **g**, NT50 values (Y-axis) vs. IgG

13

281 antibody binding (AUC, X-axis) after boost in individuals receiving two doses of an mRNA

282 vaccine. **h**, NT50 values in convalescent individuals 1.3m[3] and 6.2m[7] after infection and in

283 vaccinated individuals 2- [12] and 5-months (m) after receiving 2 doses of an mRNA vaccine. **i,**

284 NT50 values in vaccinated individuals 2-[12] and 5-months after receiving 2 doses of an mRNA

285 vaccine. Lines connect paired longitudinal samples from the same individual. **j**, Graph shows

286 NT50 values (Y-axis) vs. days (X-axis) after boost in individuals receiving two doses of an mRNA

287 vaccine. **k**, Plasma neutralizing activity against indicated SARS-CoV-2 variants of concern (n=15

288 paired samples at 2- and 5-months after full vaccination). Refer to Methods for a list of all

289 substitutions/deletions/insertions in the spike variants. All experiments were performed at least in

290 duplicate. NT50 values for Moderna mRNA-1273 and Pfizer-BioNTech BNT162b2 in **d, e, h-j**

291 are shown in black and red, respectively. Red bars and values in **e, h,** and **k** represent geometric

292 mean NT50 values. Statistical significance in **a, c, i** and **k** was determined by Wilcoxon test, in **b,**

293 **d, f, g** and **j** by spearman correlation test and in **e** and **h** by Kruskal-Wallis test with subsequent

294 Dunn's multiple comparisons.

295

14
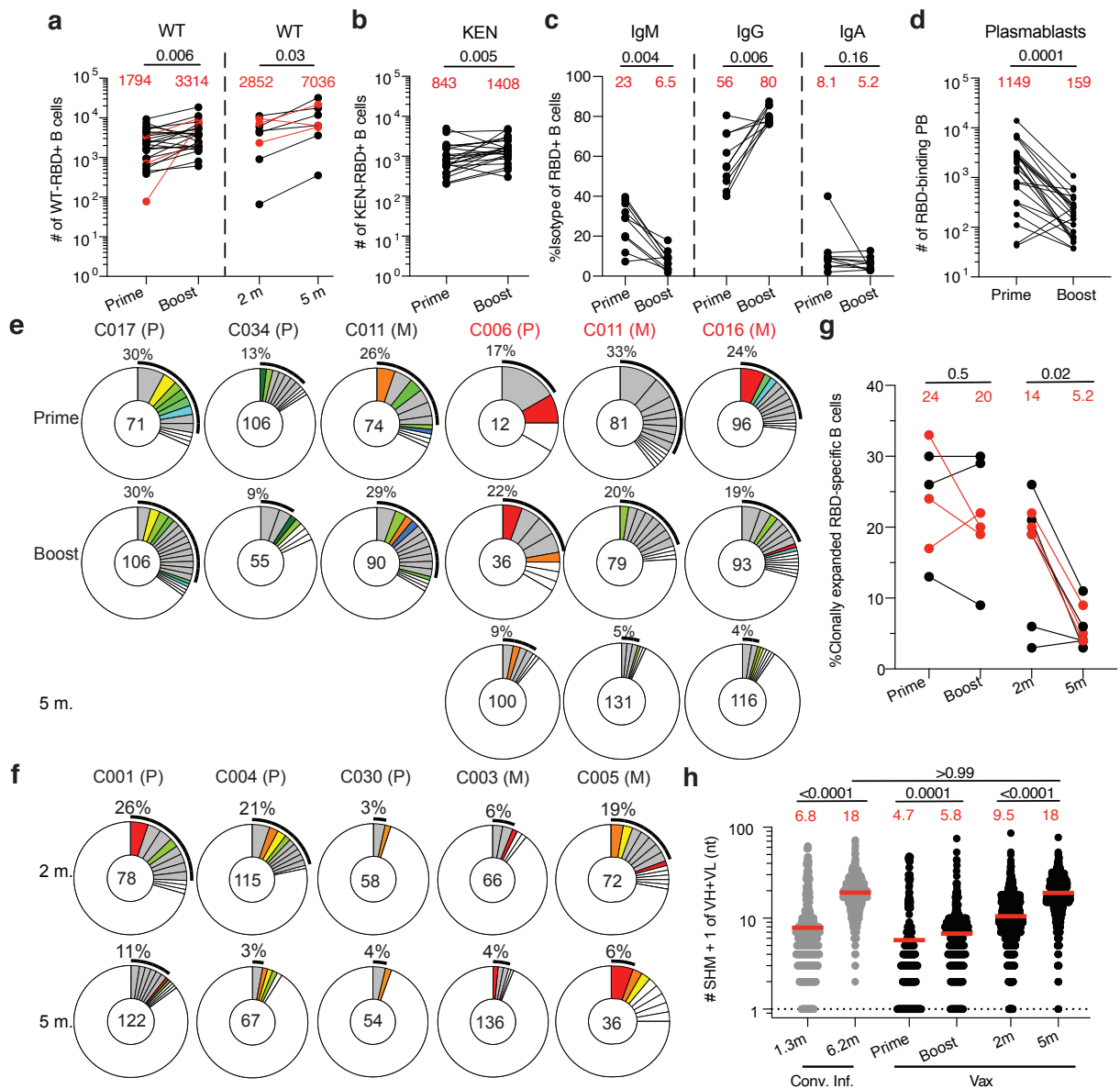
Fig. 2: Anti-SARS-CoV-2 RBD B cells after vaccination. a-d, Graphs summarizing **a,** the number of Wuhan-Hu RBD (WT)-specific memory B cells per 10 million B cells for vaccinees after prime or boost (n=26) or at follow-up of 2-[12] and 5-months after full vaccination (n=9), including 3 individuals who were sampled at prime, boost, and again 5 months post-vaccination (illustrated by red dots). **b,** the number of antigen-specific memory B cells cross-reactive with both WT and K417N/E484K/N501Y (KEN) RBD mutant per 10 million B cells after prime or boost

15

303   (n=26), **c,** the frequency of IgM, IgG, or IgA isotype expression by Wuhan-Hu RBD-specific

304   memory B cells after prime or boost (n=10), and **d,** number of Wuhan-Hu RBD-binding

305   plasmablasts per 10 million B cells (n=26) after prime or boost. Red numbers indicate geometric

306   means. Gating strategy is in Extended Data Fig. 2. **e-f,** Pie charts show the distribution of IgG

307   antibody sequences obtained from memory B cells from 11 individuals after **e,** prime or boost or

308   5-months, and **f,** 2- or 5- months. The number inside the circle indicates the number of sequences

309   analyzed for the individual denoted above the circle, with Pfizer vaccinees indicated by (P) and

310   Moderna by (M). Invidiuals in red text indicate those that were sampled at prime, boost, and again

311   5 months post-vaccination. Pie slice size is proportional to the number of clonally related

312   sequences. The black outline and associated numbers indicate the percentage of clonally expanded

313   sequences detected at each time point. Colored slices indicate persisting clones (same IGHV and

314   IGLV genes, with highly similar CDR3s) found at more than one timepoint within the same

315   individual. Grey slices indicate clones unique to the timepoint. White slices indicate repeating

316   sequences isolated only once per time point. **g,** Graph shows the relative percentage of expanded

317   clonal sequences at each time point in **e** and **f**. The red numbers indicate the geometric means. **h,**

318   Number of nucleotide mutations in the IGVH and IGVL combined (also Supplementary Table 4)

319   in the antibodies illustrated in **e** and **f**, compared to the number of mutations obtained after 1.3[3] or

320   6.2[7] months after infection (illustrated by grey dots)**.** Red horizontal bars and numbers indicate

321   mean number of nucleotide mutations at each time point. Statistical significance in **a-d** and **g** was

322   determined using Wilcoxon matched-pairs signed rank test. Statistical significance in **h** was

323   determined by Kruskal Wallis test with subsequent Dunn's multiple comparisons.

324
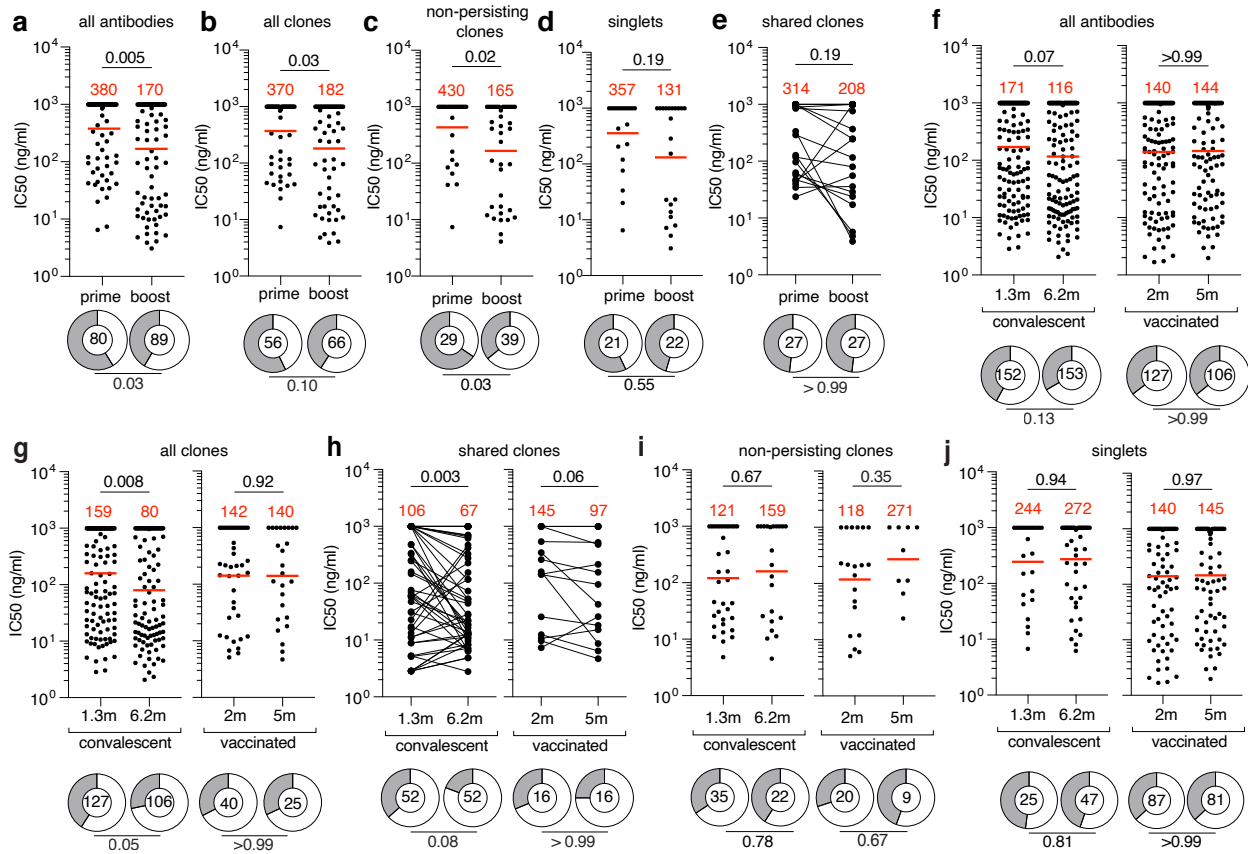
16

Fig. 3: Anti-SARS-CoV-2 RBD monoclonal antibodies. a-j, Graphs show anti-SARS-CoV-2 neutralizing activity of monoclonal antibodies measured by a SARS-CoV-2 pseudotype virus neutralization assay using wild-type (Wuhan Hu-1[47]) SARS-CoV-2 pseudovirus[3,8]. **a-e,** Half-maximal inhibitory concentration (IC_{50}) values for all antibodies (**a**), all clones (**b**), non-persisting clones (**c**), singlets (**d**) and shared clones (**e**) isolated after prime or boost. **f-j,** Half-maximal inhibitory concentration (IC_{50}) values for all antibodies (**f**), all clones (**g**), shared clones (**h**), non-persisting clones (**i**) and singlets (**j**) isolated from COVID-19 convalescent individuals 1.3^3 and 6.2^7 months after infection or from vaccinated individuals $2m^{12}$ or 5m after vaccination. Each dot represents one antibody. Pie charts illustrate the fraction of non-neutralizing ($IC50 > 1000$ ng/ml) antibodies (grey slices), inner circle shows the number of antibodies tested per group. Horizontal bars and red numbers indicate geometric mean values. Statistical significance in **a-d, f, g, i, j** was

337   determined by Mann-Whitney test and in **e** and **h** by Wilcoxon test. Statistical significance for ring

338   plots was determined using Fisher's exact test. All experiments were performed at least twice.

339

d Vaccination persisting clones 2m/5m

	wt	R683G	R346S	K417N	N440K	A475V	E484K R683G	Q493R	N501Y	KEN R683G	L452R E484Q R683G	L452R T478K R683G
C1332	5	4	8	7	6	5	5	6	5	4	4	5
C1207	103	68	121	86	125	19	61	58	26	3	61	61
C1189	113	103	129	6	112	78	5	80	77	73	8	76
C1213	101	101	14	178	164	148	52	132	133	48	100	100
C1344	77	13	77	96	66	100	93	50	82	78	78	83
C1335	48	79	73	54	68	48	86	64	50	61	141	105
C1333	86	99	97	87	89	84	95	109	93	88	92	114
C1334	65	107	173	88	109	82	99	95	66	79	112	111
C1211	115	113	165	109	188	142	122	105	126	125	130	128
C1302	85	21	70	588	64	109	77	97	102	529	78	107

%IC50 of shared clone isolated 2m after vaccination

e Convalescent infection persisting clones 1.3m/6m

	wt	R683G	R346S	K417N	N440K	A475V	E484K R683G	Q493R	N501Y	KEN R683G	L452R E484Q R683G	L452R T478K R683G
C542	2	4	2	1	2	2	1	2	1	13	1	2
C099	3	1	4	2	3	2	1	5	8	0.4	2	1
C513	16	5	19	9	10	4	15	15	15	5	4	2
C573	1	5	100	1	1	1	2	1	2	1	2	4
C043	18	2.9	17	51	13	4	1	0.3	14	2	1	3
C512	10	2	100	2	25	7	0.3	9	53	0.2	1	2
C055	2	1	2	3	2	1	42	1	1	30	1	100
C080	70	69	3	11	4	35	10	68	71	20	1	1
C549	29	6	62	38	46	44	4	1	15	34	0.1	1
C511	83	45	101	34	71	3	24	10	1	0.2	25	23
C057	47	43	38	35	30	30	89	4	22	100	0.1	31
C095	88	19	121	15	44	57	100	0.3	81	100	100	0.2
C502	154	61	169	136	97	124	100	1	126	100	100	1
C572	148	28	96	60	127	138	100	100	401	144	248	184
C051	295	49	525	293	412	241	52	1	419	100	7	34
C052	48	112	37	50	36	35	192	457	27	100	100	41

%IC50 of shared clone isolated 1.3m after infection

340

Fig. 4: Affinity and Breadth. a-c, Graphs show antibody K_{DS} for Wuhan-Hu RBD measured by BLI. **a,** antibodies isolated from vaccinees after prime (red, n=30) or boost (green, n=30). **b**, same as **a,** but from vaccinees after 2- (red, n=31) and 5-months (green, n=30). **c**, Clonal-paired antibodies isolated from convalescents 1.3[3]- and 6[7]-months after infection (n=15) or vaccinated individuals 2- and 5-months after full vaccination (n=16). Black horizontal bars and numbers indicate geometric mean values. Statistical significance was determined using two-tailed unpaired

347   t-test (**a, b**) or two tailed Kruskal Wallis test with subsequent Dunn's multiple comparisons (**c**).

348   BLI traces can be found in Extended Data Fig 7. **d-e,** Heat-maps show inhibitory concentrations

349   of antibodies isolated 5m after vaccination (**d**) or 6.2 months[7] after infection (**e**) normalized to their

350   shared clone isolated 2m after vaccination (**d**) or 1.3 months[3] after infection (**e**), expressed as

351   %IC50, against indicated mutant SARS-CoV-2 pseudoviruses (Supplementary Table 9).

352   Antibodies with improved (<30%) IC50 compared to their clonal relative isolated at an earlier

353   timepoint are colored in shades of green with most improved antibodies in darkest green.

354   Antibodies with worse (>300%) IC50 than their clonal relative isolated at an earlier timepoint are

355   colored in red with the most worsened antibodies in dark red. Antibodies that did not change their

356   IC50 by more than ~3-fold are shown in yellow.

357

358

359 **METHODS**

360

361 **Study participants**.

362 Participants were healthy volunteers receiving either the Moderna (mRNA-1273) or Pfizer-

363 BioNTech (BNT162b2) mRNA vaccines against SARS-CoV-2 who were recruited for serial blood

364 donations at Rockefeller University Hospital in New York between January 21 and June 23, 2021.

365 Participants indicated as "Prime/Boost" were individuals who were *de novo* recruited for this

366 study, while a subgroup of individuals (indicated as "2m/5m") were from a long-term study

367 cohort[12]. Eligible participants were healthy adults with no history of infection with SARS-CoV-2,

368 as determined by clinical history and confirmed through serology testing, receiving one of the two

369 Moderna (mRNA-1273) or Pfizer-BioNTech (BNT162b2), according to current dosing and

370 interval guidelines. Exclusion criteria included incomplete vaccination status, presence of clinical

371 signs and symptoms suggestive of acute infection with or a positive RT-PCR results for SARS-

372 CoV-2 in saliva, or a positive COVID-19 serology. Seronegativity for COVID-19 was established

373 through the absence of serological activity toward the nucleocapsid protein (N) of SARS-CoV-2.

374 Participants presented to the Rockefeller University Hospital for blood sample collection and were

375 asked to provide details of their vaccination regimen, possible side effects, comorbidities and

376 possible COVID-19 history. All participants provided written informed consent before

377 participation in the study and the study was conducted in accordance with Good Clinical Practice.

378 The study was performed in compliance with all relevant ethical regulations and the protocol

379 (DRO-1006) for studies with human participants was approved by the Institutional Review Board

380 of the Rockefeller University. For detailed participant characteristics see Supplementary Tables 1

381 and 2.

382

Blood samples processing and storage.

384 Peripheral Blood Mononuclear Cells (PBMCs) obtained from samples collected at Rockefeller

385 University were purified as previously reported by gradient centrifugation and stored in liquid

386 nitrogen in the presence of FCS and DMSO[3,7]. Heparinized plasma and serum samples were

387 aliquoted and stored at -20°C or less. Prior to experiments, aliquots of plasma samples were heat-

388 inactivated (56°C for 1 hour) and then stored at 4°C.

389

ELISAs

391 ELISAs[48,49] to evaluate antibodies binding to SARS-CoV-2 RBD were performed by coating of

392 high-binding 96-half-well plates (Corning 3690) with 50 μl per well of a 1μg/ml protein solution

393 in PBS overnight at 4 °C. Plates were washed 6 times with washing buffer (1× PBS with 0.05%

394 Tween-20 (Sigma-Aldrich)) and incubated with 170 μl per well blocking buffer (1× PBS with

395 2% BSA and 0.05% Tween-20 (Sigma)) for 1 h at room temperature. Immediately after

396 blocking, monoclonal antibodies or plasma samples were added in PBS and incubated for 1 h at

397 room temperature. Plasma samples were assayed at a 1:66 starting dilution and 10 additional

398 threefold serial dilutions. Monoclonal antibodies were tested at 10 μg/ml starting concentration

399 and 10 additional fourfold serial dilutions. Plates were washed 6 times with washing buffer and

400 then incubated with anti-human IgG, IgM or IgA secondary antibody conjugated to horseradish

401 peroxidase (HRP) (Jackson Immuno Research 109-036-088 109-035-129 and Sigma A0295) in

402 blocking buffer at a 1:5,000 dilution (IgM and IgG) or 1:3,000 dilution (IgA). Plates were

403 developed by addition of the HRP substrate, TMB (ThermoFisher) for 10 min (plasma samples)

404 or 4 minutes (monoclonal antibodies). The developing reaction was stopped by adding 50 μl of 1

405   M H_2SO_4 and absorbance was measured at 450 nm with an ELISA microplate reader (FluoStar

406   Omega, BMG Labtech) with Omega and Omega MARS software for analysis. For plasma

407   samples, a positive control (plasma from participant COV72, diluted 66.6-fold and ten additional

408   threefold serial dilutions in PBS) was added to every assay plate for validation. The average of

409   its signal was used for normalization of all the other values on the same plate with Excel

410   software before calculating the area under the curve using Prism V9.1(GraphPad). For

411   monoclonal antibodies, the EC50 was determined using four-parameter nonlinear regression

412   (GraphPad Prism V9.1). EC50s above 2000 ng/mL were considered non-binders.

413

414   **Proteins**

415   Mammalian expression vector encoding the RBD of SARS-CoV-2 (GenBank MN985325.1; S

416   protein residues 319-539) was previously described[50].

417

418   **SARS-CoV-2 pseudotyped reporter virus**

419   A panel of plasmids expressing RBD-mutant SARS-CoV-2 spike proteins in the context of

420   pSARS-CoV-2-S $_{\Delta 19}$ has been described[12,22,51]. Variant pseudoviruses resembling variants of

421   concern B.1.1.7 (first isolated in the UK), B.1.351 (first isolated in South-Africa), B.1.526 (first

422   isolated in New York City), P.1 (first isolated in Brazil) and B.1.617.2 (first isolated in India)

423   were generated by introduction of substitutions using synthetic gene fragments (IDT) or overlap

424   extension PCR mediated mutagenesis and Gibson assembly. Specifically, the variant-specific

425   deletions and substitutions introduced were:

426   B.1.1.7: ΔH69/V70, ΔY144, N501Y, A470D, D614G, P681H, T761I, S982A, D118H

427   B.1.351: D80A, D215G, L242H, R246I, K417N, E484K, N501Y, D614G, A701V

23

428 B.1.526: L5F, T95I, D253G, E484K, D614G, A701V.

429 P.1: L18F, T20N, P26S, D138Y, R190S, K417T, E484K, N501Y, D614G, H655Y, T1027I,

430 V1167F

431 B.1.617.2: T19R, Δ156-158, L452R, T478K, D614G, P681R, D950N

432 The E484K, K417N/E484K/N501Y (KEN), L452R/E484Q and L452R/T478K substitution, as

433 well as the deletions/substitutions corresponding to variants of concern listed above were

434 incorporated into a spike protein that also includes the R683G substitution, which disrupts the

435 furin cleaveage site and increases particle infectivity. Neutralizing activity against mutant

436 pseudoviruses were compared to a wildtype SARS-CoV-2 spike sequence (NC_045512),

437 carrying R683G where appropriate.

438

439 SARS-CoV-2 pseudotyped particles were generated as previously described[3,8]. Briefly, 293T

440 cells were transfected with pNL4-3ΔEnv-nanoluc and pSARS-CoV-2-S$_{\Delta 19}$, particles were

441 harvested 48 hpt, filtered and stored at -80°C.

442

443 **Pseudotyped virus neutralization assay**

444 Fourfold serially diluted plasma from COVID-19-convalescent individuals or monoclonal

445 antibodies were incubated with SARS-CoV-2 pseudotyped virus for 1 h at 37 °C. The mixture

446 was subsequently incubated with 293T$_{Ace2}$ cells[3] (for all WT neutralization assays) or

447 HT1080Ace2 cl14 (for all mutant panels and variant neutralization assays) cells[12] for 48h after

448 which cells were washed with PBS and lysed with Luciferase Cell Culture Lysis 5× reagent

449 (Promega). Nanoluc Luciferase activity in lysates was measured using the Nano-Glo Luciferase

450 Assay System (Promega) with the Glomax Navigator (Promega). The relative luminescence units

24

451   were normalized to those derived from cells infected with SARS-CoV-2 pseudotyped virus in the

452   absence of plasma or monoclonal antibodies. The half-maximal neutralization titers for plasma

453   (NT_{50}) or half-maximal and 90% inhibitory concentrations for monoclonal antibodies (IC_{50} and

454   IC_{90}) were determined using four-parameter nonlinear regression (least squares regression

455   method without weighting; constraints: top=1, bottom=0) (GraphPad Prism).

456

457   **Biotinylation of viral protein for use in flow cytometry**

458   Purified and Avi-tagged SARS-CoV-2 RBD or SARS-CoV-2 RBD KEN mutant (K417N,

459   E484K, N501Y) was biotinylated using the Biotin-Protein Ligase-BIRA kit according to

460   manufacturer's instructions (Avidity) as described before[3]. Ovalbumin (Sigma, A5503-1G) was

461   biotinylated using the EZ-Link Sulfo-NHS-LC-Biotinylation kit according to the manufacturer's

462   instructions (Thermo Scientific). Biotinylated ovalbumin was conjugated to streptavidin-BV711

463   (BD biosciences, 563262) and RBD to streptavidin-PE (BD Biosciences, 554061) and

464   streptavidin-AF647 (Biolegend, 405237)[3].

465

466   **Flow cytometry and single cell sorting**

467   Single-cell sorting by flow cytometry was described previously[3]. Briefly, peripheral blood

468   mononuclear cells were enriched for B cells by negative selection using a pan-B-cell isolation kit

469   according to the manufacturer's instructions (Miltenyi Biotec, 130-101-638). The enriched B

470   cells were incubated in FACS buffer (1× PBS, 2% FCS, 1 mM EDTA) with the following anti-

471   human antibodies (all at 1:200 dilution): anti-CD20-PECy7 (BD Biosciences, 335793), anti-

472   CD3-APC-eFluro 780 (Invitrogen, 47-0037-41), anti-CD8-APC-eFluor 780 (Invitrogen, 47-

473   0086-42), anti-CD16-APC-eFluor 780 (Invitrogen, 47-0168-41), anti-CD14-APC-eFluor 780

474 (Invitrogen, 47-0149-42), as well as Zombie NIR (BioLegend, 423105) and fluorophore-labelled

475 RBD and ovalbumin (Ova) for 30 min on ice. Single CD3-CD8-CD14-CD16−CD20+Ova−RBD-

476 PE+RBD-AF647+ B cells were sorted into individual wells of 96-well plates containing 4 µl of

477 lysis buffer (0.5× PBS, 10 mM DTT, 3,000 units/ml RNasin Ribonuclease Inhibitors (Promega,

478 N2615) per well using a FACS Aria III and FACSDiva software (Becton Dickinson) for

479 acquisition and FlowJo for analysis. The sorted cells were frozen on dry ice, and then stored at

480 −80 °C or immediately used for subsequent RNA reverse transcription. For plasmablast single-

481 cell sorting, in addition to above antibodies, B cells were also stained with anti-CD19-BV605

482 (Biolegend, 302244), and single CD3-CD8-CD14-CD16-CD19+CD20-Ova-RBD-PE+RBD-

483 AF647+ plasmablasts were sorted as described above. For B cell phenotype analysis, in addition

484 to above antibodies, B cells were also stained with following anti-human antibodies: anti-IgD-

485 BV421 (Biolegend, 348226), anti-CD27-FITC (BD biosciences, 555440), anti-CD19-BV605

486 (Biolegend, 302244), anti-CD71- PerCP-Cy5.5 (Biolegend, 334114), anti- IgG-PECF594 (BD

487 biosciences, 562538), anti-IgM-AF700 (Biolegend, 314538), anti-IgA-Viogreen (Miltenyi

488 Biotec, 130-113-481).

489

490 **Antibody sequencing, cloning and expression**

491 Antibodies were identified and sequenced as described previously[3,52]. In brief, RNA from single

492 cells was reverse-transcribed (SuperScript III Reverse Transcriptase, Invitrogen, 18080-044) and

493 the cDNA was stored at −20 °C or used for subsequent amplification of the variable IGH, IGL

494 and IGK genes by nested PCR and Sanger sequencing. Sequence analysis was performed using

495 MacVector. Amplicons from the first PCR reaction were used as templates for sequence- and

496   ligation-independent cloning into antibody expression vectors. Recombinant monoclonal

497   antibodies were produced and purified as previously described[3].

498

499   **Biolayer interferometry**

500   Biolayer interferometry assays were performed as previously described[3]. Briefly, we used the

501   Octet Red instrument (ForteBio) at 30 °C with shaking at 1,000 r.p.m. Affinity measurement of

502   anti-SARS-CoV-2 IgGs binding were corrected by subtracting the signal obtained from traces

503   performed with IgGs in the absence of WT RBD. The kinetic analysis using protein A biosensor

504   (ForteBio 18-5010) was performed as follows: (1) baseline: 60sec immersion in buffer. (2)

505   loading: 200sec immersion in a solution with IgGs 10 μg/ml. (3) baseline: 200sec immersion in

506   buffer. (4) Association: 300sec immersion in solution with WT RBD at 20, 10 or 5 μg/ml (5)

507   dissociation: 600sec immersion in buffer. Curve fitting was performed using a fast 1:1 binding

508   model and the Data analysis software (ForteBio). Mean KD values were determined by

509   averaging all binding curves that matched the theoretical fit with an R^2 value ≥ 0.8.

510

511   **Computational analyses of antibody sequences**

512   Antibody sequences were trimmed based on quality and annotated using Igblastn v.1.14. with

513   IMGT domain delineation system. Annotation was performed systematically using Change-O

514   toolkit v.0.4.540[53]. Heavy and light chains derived from the same cell were paired, and

515   clonotypes were assigned based on their V and J genes using in-house R and Perl scripts. All

516   scripts and the data used to process antibody sequences are publicly available on GitHub

517   (https://github.com/stratust/igpipeline/tree/igpipeline2_timepoint_v2).

518

519   The frequency distributions of human V genes in anti-SARS-CoV-2 antibodies from this study

520   was compared to 131,284,220 IgH and IgL sequences generated by[54] and downloaded from cAb-

521   Rep[55], a database of human shared BCR clonotypes available at https://cab-

522   rep.c2b2.columbia.edu/. Based on the 112 distinct V genes that make up the 7936 analyzed

523   sequences from Ig repertoire of the 11 participants present in this study, we selected the IgH and

524   IgL sequences from the database that are partially coded by the same V genes and counted them

525   according to the constant region. The frequencies shown in Extended Data Fig. 4 are relative to

526   the source and isotype analyzed. We used the two-sided binomial test to check whether the

527   number of sequences belonging to a specific IgHV or IgLV gene in the repertoire is different

528   according to the frequency of the same IgV gene in the database. Adjusted p-values were

529   calculated using the false discovery rate (FDR) correction. Significant differences are denoted

530   with stars.

531

532   Nucleotide somatic hypermutation and CDR3 length were determined using in-house R and Perl

533   scripts. For somatic hypermutations, IGHV and IGLV nucleotide sequences were aligned against

534   their closest germlines using Igblastn and the number of differences were considered nucleotide

535   mutations. The average number of mutations for V genes was calculated by dividing the sum of

536   all nucleotide mutations across all participants by the number of sequences used for the analysis.

537

538   **Data availability statement:** Data are provided in Supplementary Tables 1-9. The raw

539   sequencing data and computer scripts associated with Figure 2 and Extended Data Fig. 3 have

540   been deposited at Github (https://github.com/stratust/igpipeline/tree/igpipeline2_timepoint_v2).

541   This study also uses data from "A Public Database of Memory and Naive B-Cell Receptor

28

542   Sequences" (https://doi.org/10.5061/dryad.35ks2), PDB (6VYB and 6NB6) and from "High

543   frequency of shared clonotypes in human B cell receptor repertoires"

544   (https://doi.org/10.1038/s41586-019-0934-8).

545

546   **Code availability statement:** Computer code to process the antibody sequences is available at

547   GitHub (https://github.com/stratust/igpipeline/tree/igpipeline2_timepoint_v2).

548
549

550   **Data presentation**

551   Figures arranged in Adobe Illustrator 2020.

552

553   **Competing interests:** The Rockefeller University has filed a provisional patent application in

554   connection with this work on which M.C.N.is an inventor (US patent 63/021,387). The patent

555   has been licensed by Rockefeller University to Bristol Meyers Squib.

556

570   **Author Contributions:** P.D.B., T.H., and M.C.N. conceived, designed and analyzed

571   the experiments. M. Caskey and C.G. designed clinical protocols. A.C, F.M., D.S.B., Z.W., S.F.

572   M.A., E.B., J.D.S., I.S., J.D. F.S., F.Z., and T.B.T. carried out experiments. A.G. and M. Cipolla

573   produced antibodies. D.S.B., M.D., M.T., K.G.M., C.G. and M. Caskey recruited participants,

574   executed clinical protocols. T.Y.O. and V.R. performed bioinformatic analysis. A.C., F.M,

575   D.S.B., Z.W., S.F., and M.C.N. wrote the manuscript with input from all co-authors.

576

577

578 **EXTENDED FIGURES**
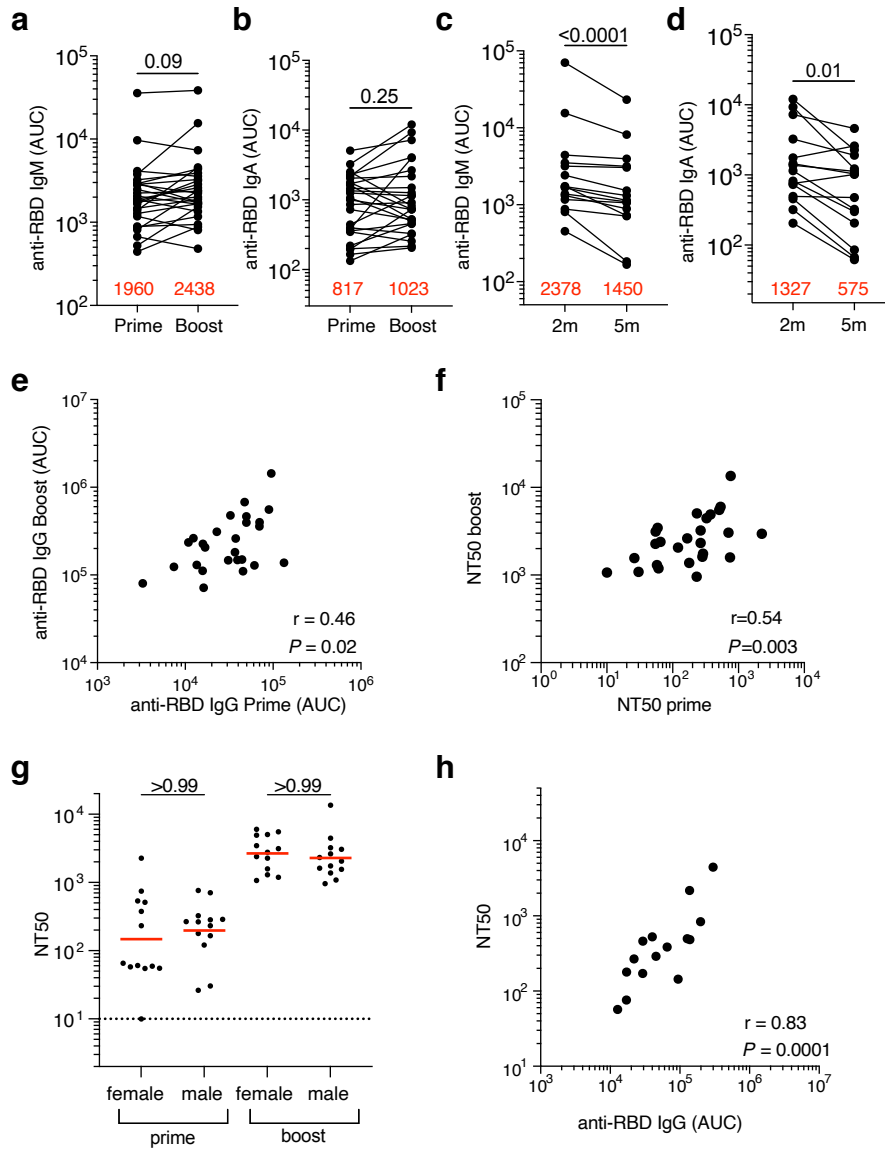
579

580 **Extended Data Fig 1: Plasma ELISA and neutralization.**

581 **a,b,** Graph shows area under the curve (AUC, Y-axis) for plasma IgM (**a**) or IgA (**b**) antibody

582 binding to SARS-CoV-2 RBD after prime and boost for paired samples. **c,d,** Graph shows area

583 under the curve (AUC, Y-axis) for plasma IgM (**c**) or IgA (**d**) antibody binding to SARS-CoV-2

584 RBD of paired samples obtained 2 and 5 months after the boost. **e,f,** IgG antibody binding (AUC,

585 X-axis) after prime vs. IgG antibody binding (AUC, X-axis) after boost (**e**) and NT50 values after

31

586   prime vs. NT50 values after boost (**f**) in individuals receiving two doses of an mRNA vaccine. **g,**

587   NT50 values after prime and boost in females and males receiving 2 doses of an mRNA vaccine.

588   **h,** NT50 values (Y-axis) vs. IgG antibody binding (AUC, X-axis) 5 months after boost in

589   individuals receiving two doses of an mRNA vaccine. All experiments were performed at least in

590   duplicate. Red values or bar in **a-d** and **g** represent geometric mean values. Statistical significance

591   in **a-d** was determined by Wilcoxon test, in **e, f, and h** by spearman correlation test and in **g** by

592   Kruskall-Wallis test with subsequent Dunn's multiple comparisons.

593

594

33
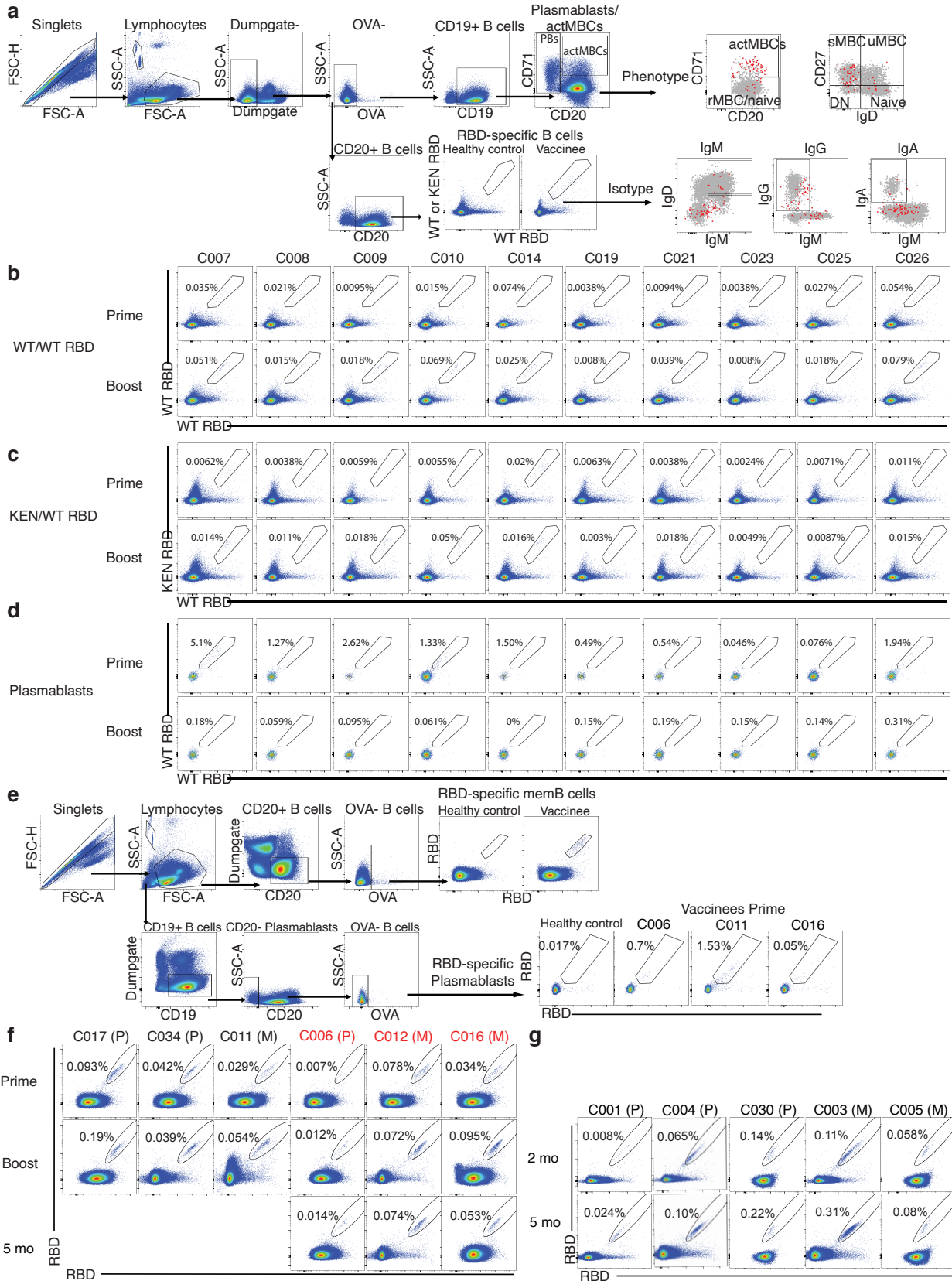
595   **Extended Data Fig. 2: Flow Cytometry. a,** Gating strategy for phenotyping. Gating was on

596   singlets that were CD19$^+$ or CD20$^+$ and CD3-CD8-CD16-Ova-. Anti-IgG, IgM, IgA, IgD, CD71

597   and CD27 antibodies were used for B cell phenotype analysis. Antigen-specific cells were detected

598   based on binding to RBD WT-PE$^+$ and RBD WT/KEN-AF647$^+$. **b-d,** Flow cytometry plots

599   showing the frequency of **b,** RBD WT-binding memory B cells, and **c,** RBD-binding memory B

600   cells cross-reactive with WT and K417N/E484K/N501Y mutant RBD and **d,** RBD-binding

601   plasmablasts, in 10 selected vaccinees after prime or boost. **e,** Gating strategy for single-cell sorting

602   for CD20+ memory B cells (top panel) or CD19+CD20- plasmablasts (bottom panel) which were

603   double positive for RBD-PE and RBD-AF647. **f-g,** Representative flow cytometry plots showing

604   dual AlexaFluor-647-RBD and PE-RBD-binding, single-cell sorted B cells from **f,** 6 individuals

605   after prime or boost or 5 months post-vaccination and **g,** 5 individuals from 2- or 5-months post-

606   vaccination. Percentage of RBD-specific B cells is indicated. Invidiuals in red text indicate those

607   that were sampled at prime, boost, and again 5 months post-vaccination.

608
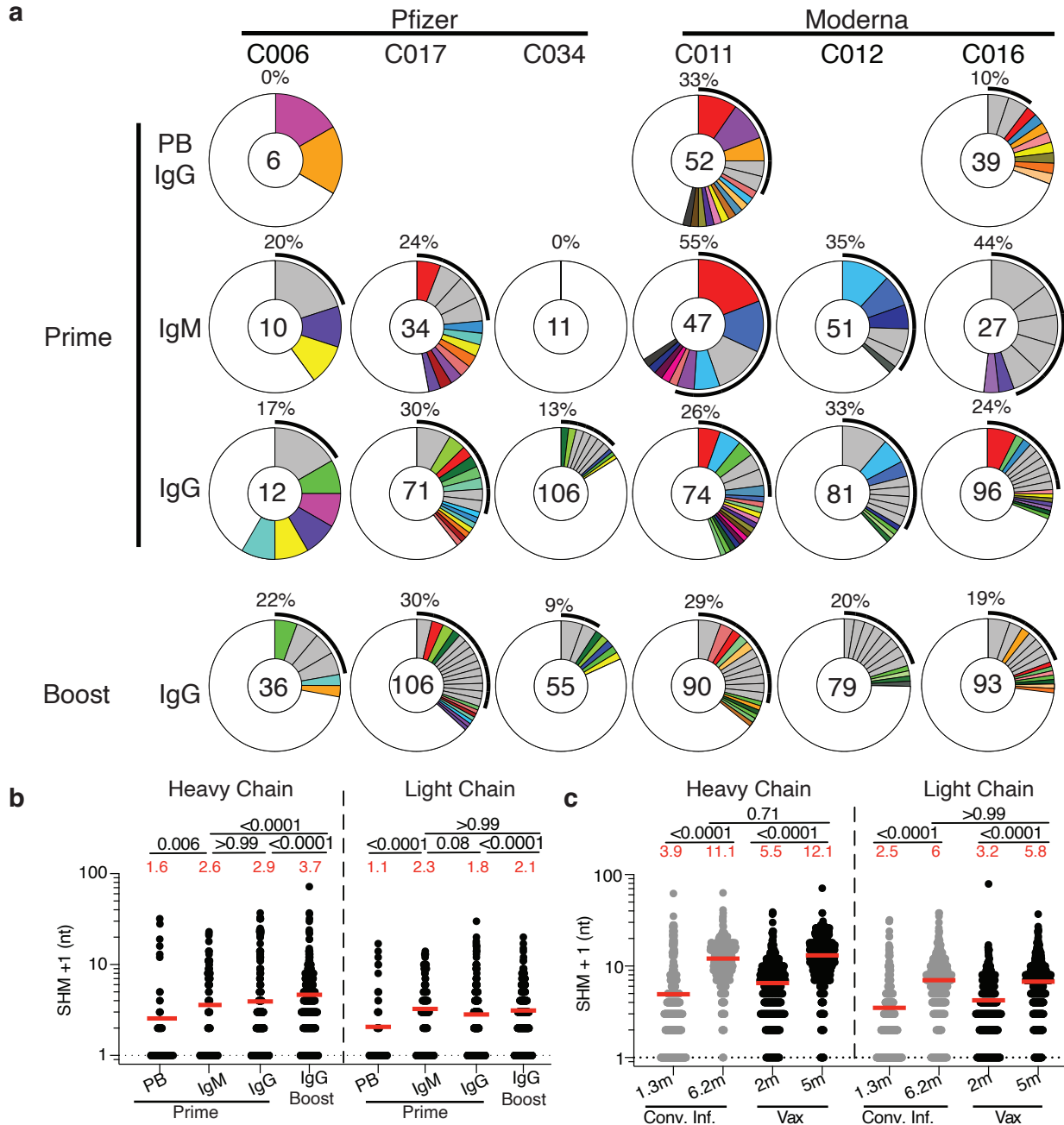
Extended Data Fig 3: anti-SARS-CoV-2 RBD-specific plasmablast and MBC responses after

vaccination. a, Pie charts show the distribution of antibody sequences from 6 individuals after

prime (upper panel) or boost (lower panel). Sequences derived from IgG plasmablast, IgM MBC,

and IgG MBC compartments were analyzed after prime, while only IgG MBCs were analyzed

after boost, as indicated to the left of the plots. The number inside the circle indicates the number

615   of sequences analyzed for the individual denoted above the circle. Pie slice size is proportional to

616   the number of clonally related sequences. The black outline indicates the frequency of clonally

617   expanded sequences detected in each patient. Colored slices indicate persisting clones (same IGHV

618   and IGLV genes, with highly similar CDR3s) found in multiple compartments and/or timepoints

619   within the same patient. Grey slices indicate clones unique to the compartment. White indicates

620   sequences isolated once. **b-c,** Number of somatic nucleotide mutations in the IGVH and IGVL,

621   separately, in antibodies detected in **b,** different B cell compartments after prime or boost and **c,**

622   2^{12} or 5 months post-vaccination compared to convalescent infected individuals after 1.3^{3} and 6.2^{7}

623   months post-infection (also Supplementary Table 4). Red horizontal bars and numbers indicate

624   mean number of nucleotide mutations in each compartment at each time point. Statistical

625   significance was determined using a Kruskal Wallis test with subsequent Dunn's multiple

626   comparisons.

627
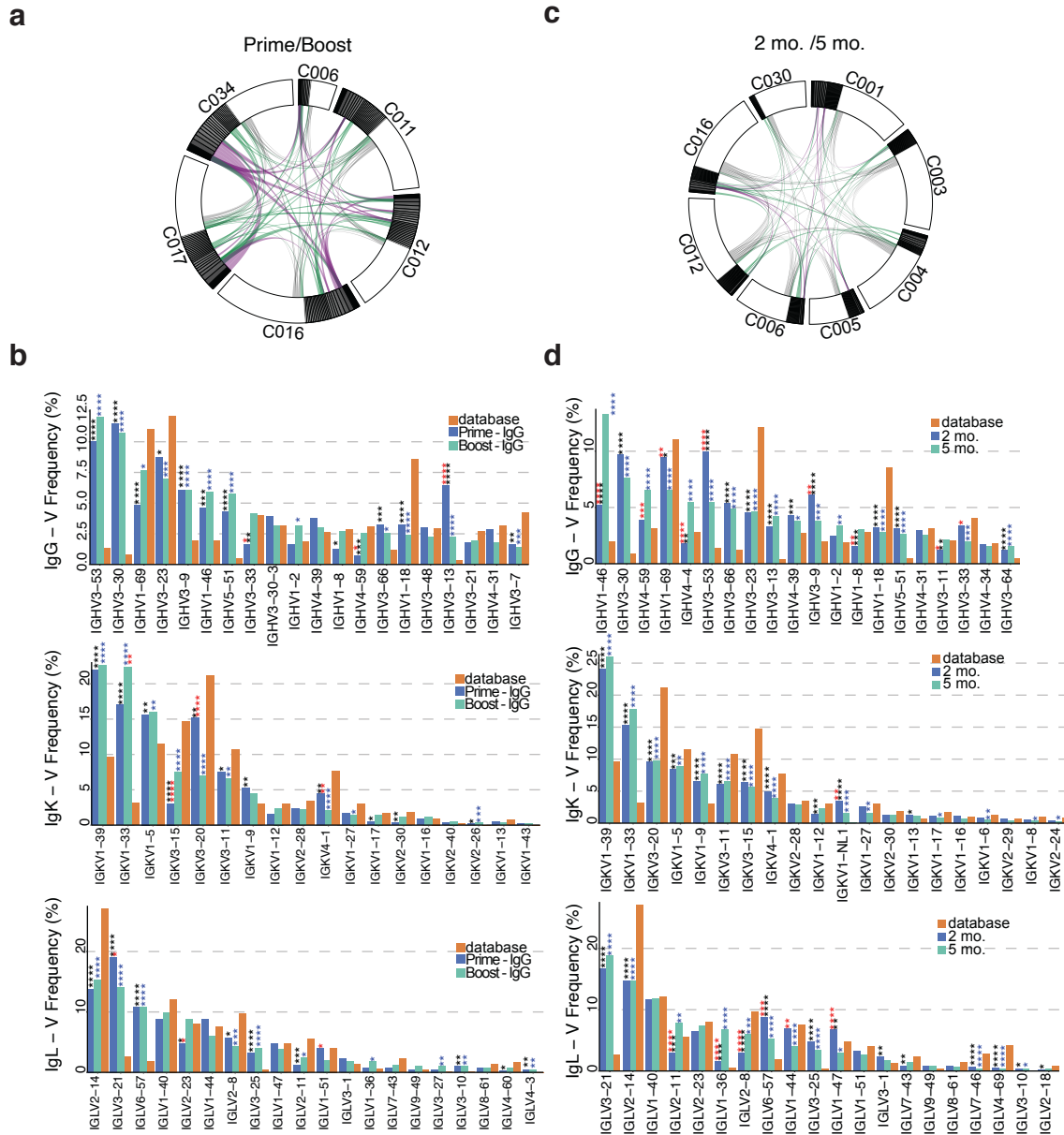
Extended Data Fig. 4: Frequency distribution of human V genes. a, Circos plot depicting relationship between antibodies that share V and J gene usage in both IgH and IgL when comparing all prime/boost IgG MBC sequences. Purple, green, and grey lines connect related clones, clones and singlets, and singlets to each other, respectively. **b,** Graph shows relative abundance of human heavy chain IGVH (top), light chain IGVK (middle) or IGVL (bottom) genes comparing Sequence Read Archive accession SRP010970 (orange), and IgG MBCs after prime (blue) or boost (green)

635   doses of vaccination. Statistical significance was determined by two-sided binomial test. * =

636    $p \leq 0.05$, ** = $p \leq 0.01$, *** = $p \leq 0.001$, **** = $p \leq 0.0001$. Color of stars indicates: black - comparing

637   Database versus Prime; blue - comparing Database versus Boost; red - comparing Prime versus

638   Boost. **c,** Circos plot depicting relationship between antibodies that share V and J gene usage in

639   both IgH and IgL when comparing 2 mo/5 mo IgG MBC sequences. Purple, green, and grey lines

640   connect related clones, clones and singlets, and singlets to each other, respectively. **d,** Graph shows

641   relative abundance of human heavy chain IGVH (top), light chain IGVK (middle) or IGVL

642   (bottom) genes comparing Sequence Read Archive accession SRP010970 (orange), and IgG

643   MBCs after 2 months (blue) or 5 months (green) post-vaccination. Statistical significance was

644   determined by two-sided binomial test. * = $p \leq 0.05$, ** = $p \leq 0.01$, *** = $p \leq 0.001$, **** = $p \leq 0.0001$.

645   Color of stars indicates: black - comparing Database versus 2 months; blue - comparing Database

646   versus 5 months; red - comparing 2 months versus 5 months.

647

648
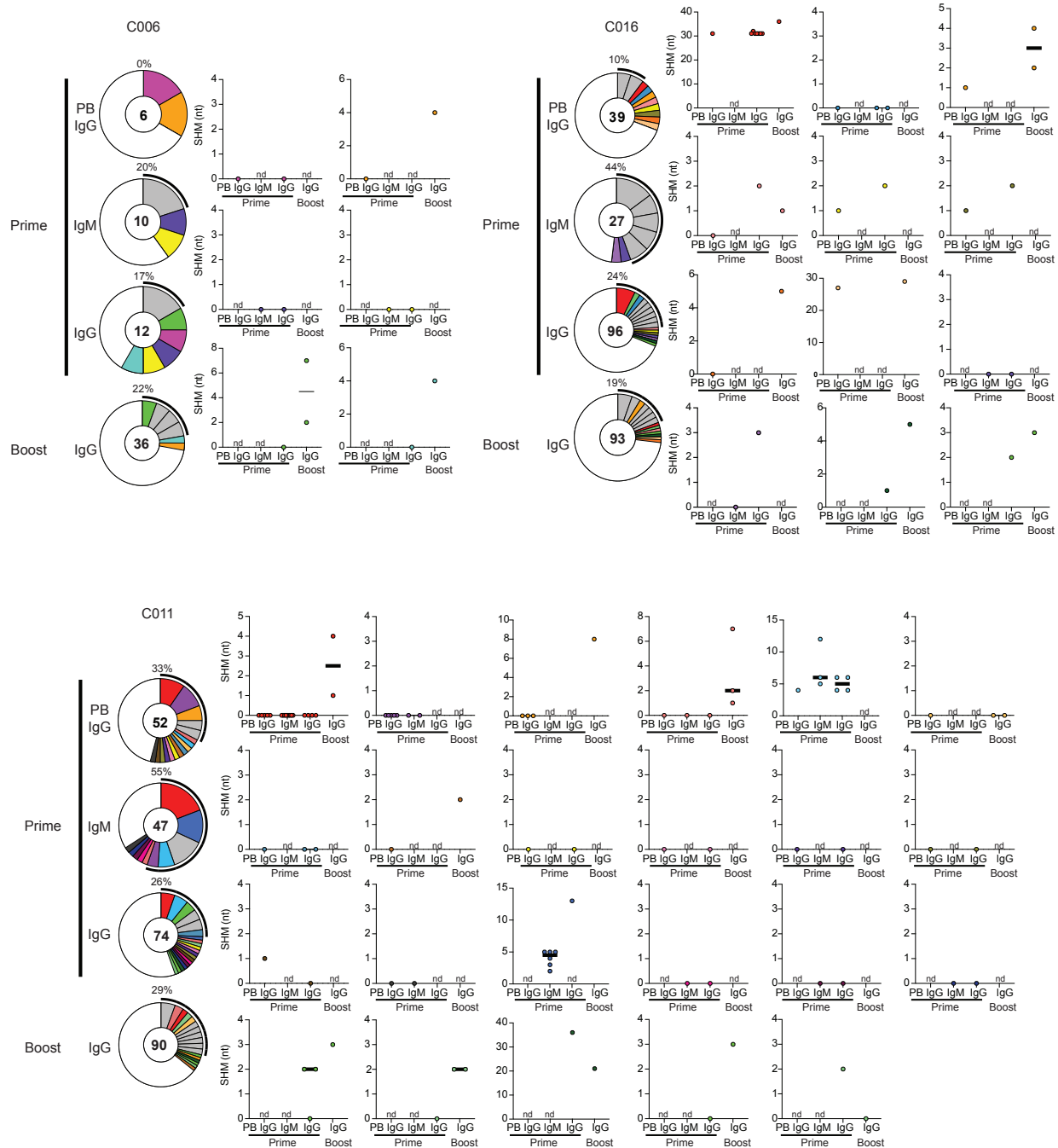
Extended Data Fig. 5: Somatic hypermutation of anti-SARS-CoV-2 RBD antibody clones

after prime or boost. Clonal evolution of RBD-binding B cells from 3 individuals for which

plasmablasts, IgM memory B cells, and IgG memory B cells were analyzed after prime, and IgG

memory B cells were analyzed after boost (as described in Extended Data Fig. 3). The number of

653   somatic nucleotide mutations found in shared clonal families found in at least 2 different

654   compartments is graphed to the right of each donut plot. Color of dot plots match the color of pie

655   slices within the donut plot, which indicate persisting clones. nd – clone was Not Detected in the

656   indicated compartment. Black horizontal line indicates median number of SHM.

657
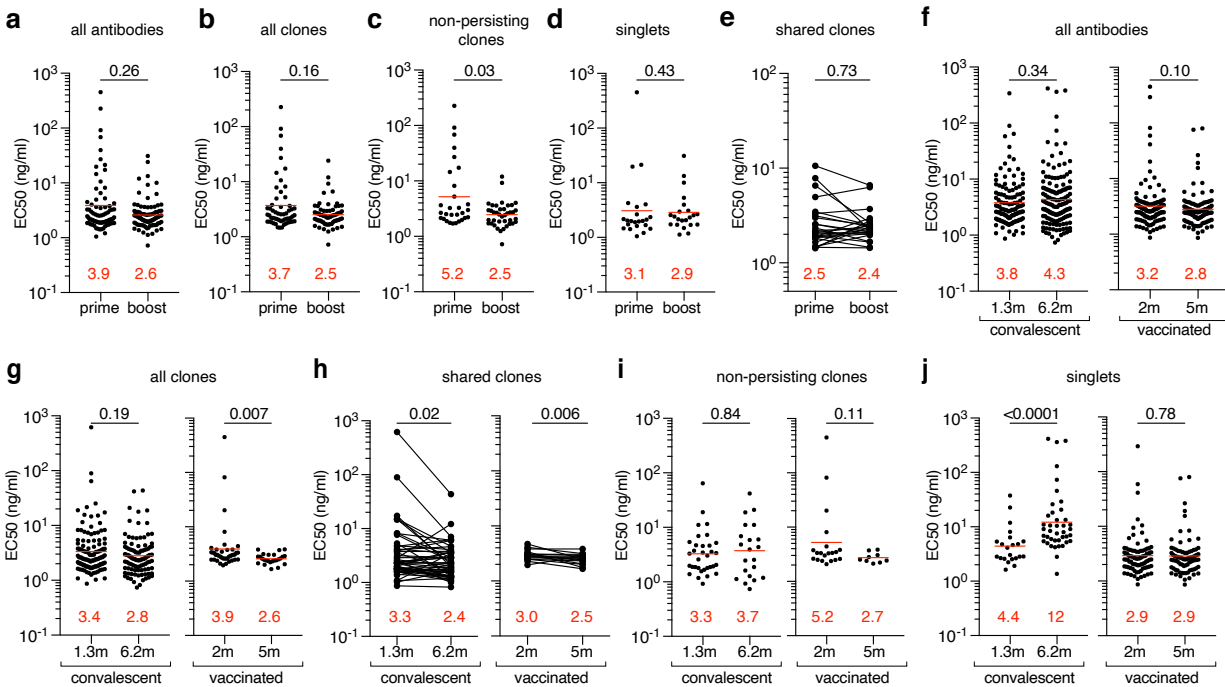
Extended Data Fig. 6: Anti-SARS-CoV-2 RBD monoclonal antibodies ELISAs. a-j, Graphs show anti-SARS-CoV-2 binding activity of monoclonal antibodies measured by ELISA against RBD. **a-e,** ELISA half-maximal concentration (EC_{50}) values for all antibodies (**a**), all clones (**b**), non-persisting clones (**c**), singlets (**d**) and shared clones (**e**) isolated after prime or boost. **f-j,** ELISA half-maximal concentration (EC_{50}) values for all antibodies (**f**), all clones (**g**), shared clones (**h**), non-persisting clones (**i**) and singlets (**j**) isolated from COVID-19 convalescent individuals 1.3[3] and 6.2[7] months after infection or from vaccinated individuals 2m[12] or 5m after vaccination. Each dot represents one antibody. Red horizontal bars and numbers indicate geometric mean values. Statistical significance in **a-d, f, g, i, j** was determined by Mann-Whitney test and in **e** and **h** by Wilcoxon test. All experiments were performed at least twice.
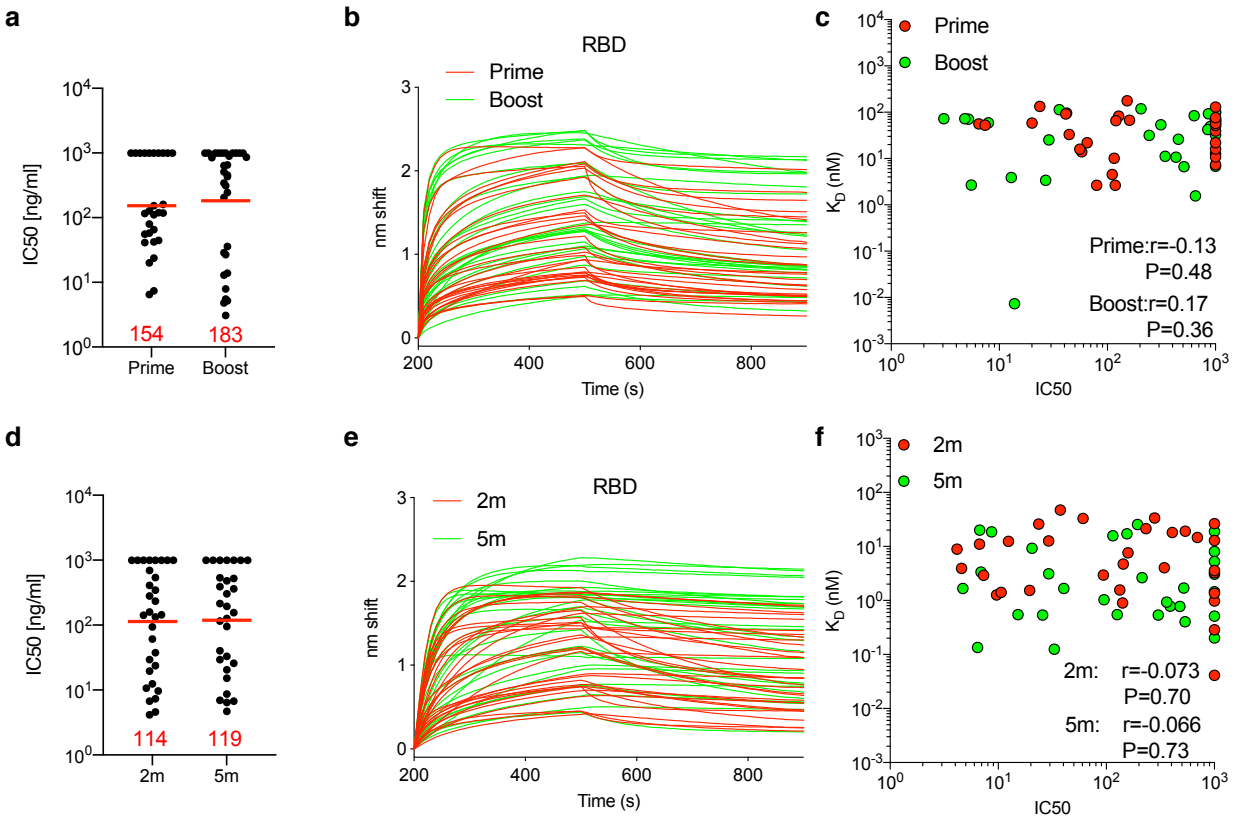
Extended Data Fig. 7. Affinity. Biolayer interferometry measurements. **a**, IC50 values for randomly selected antibodies isolated from vaccinees after prime (n=30) of boost (n=30). Red horizontal lines and numbers indicate geometric mean. **b,** Graphs depict affinity measurements of antibodies described in **a. c,** Graphs show affinities (Y axis) plotted against neutralization activity (X axis) for antibody isolated after vaccination. **d-f,** same as in **a-c,** but showing monoclonal antibodies isolated from follow-up of 2 and 5 months post-vaccination. **d,** IC50 values for randomly selected antibodies isolated from vaccinees after 2- (n=31) or 5- (n=30) months post-vaccination. **e**, Graphs depicting affinity measurements of antibodies described in **d. f,** Graph shows affinity (Y axis) plotted against neutralization activity (X axis) for antibody isolated after vaccination.

42

a

	wt	R683G	R346S	K417N	N440K	A475V	E484K R683G	Q493R	N501Y	KEN R683G	L452R E484Q R683G
C2159	12.2	6.2	9.1	3.3	11.2	8.8	627.1	17.1	20.6	212.0	36.9
C2029	25.1	7.6	>1000	5.9	23.0	19.5	1.8	14.6	57.7	1.6	>1000
C2139	46.0	25.4	33.0	>1000	48.7	>1000	153.6	>1000	>1000	>1000	105.1
C2033	46.2	25.8	32.0	>1000	41.4	868.4	79.5	183.4	668.2	>1000	52.1
C2209	52.6	26.7	40.7	12.5	48.2	214.0	107.3	341.9	214.9	58.8	44.0
C2020	65.8	37.8	164.0	>1000	53.5	71.5	131.3	>1000	119.0	>1000	83.7
C2221	69.3	26.4	47.6	>1000	58.8	>1000	355.2	>1000	46.3	>1000	124.0
C2019	88.5	96.3	>1000	25.5	90.8	70.1	726.4	92.3	125.5	380.3	>1000
C2110	118.4	106.6	92.6	>1000	109.9	797.4	254.9	198.0	301.5	>1000	218.3
C2018	118.9	37.2	55.4	33.4	110.8	98.0	284.5	123.8	135.8	140.0	>1000
C2022	153.4	61.6	114.5	>1000	130.5	>1000	247.7	358.7	162.8	>1000	139.2
C2113	348.4	127.8	242.4	166.8	267.1	347.9	>1000	922.3	339.4	>1000	>1000
C2149	376.8	178.6	259.3	>1000	331.2	>1000	724.8	>1000	>1000	>1000	608.0
C2026	433.1	25.6	258.1	400.1	350.5	925.7	188.0	368.0	387.1	190.1	147.3
C2150	591.0	57.5	672.9	496.9	413.7	783.8	240.8	406.4	543.2	202.1	199.1
C2013	593.3	204.6	391.0	>1000	484.3	117.9	>1000	>1000	>1000	>1000	>1000
C2185	670.6	116.1	440.0	239.1	494.6	818.2	412.8	759.7	485.4	246.7	251.1
C2004	722.5	117.4	529.5	521.1	468.7	>1000	400.1	496.2	928.0	318.2	345.1
C2140	840.9	124.4	706.9	839.5	778.2	>1000	648.7	866.7	815.5	481.7	497.8
C2109	1000.0	198.7	572.6	825.0	336.9	>1000	960.0	762.2	620.2	691.7	464.7

IC50 (ng/ml)

b

	wt	R683G	R346S	K417N	N440K	A475V	E484K R683G	Q493R	N501Y	KEN R683G	L452R E484Q R683G
C2039	1.9	0.5	1.0	0.7	1.2	1.0	>1000	1.4	2.3	>1000	>1000
C2237	6.7	0.7	3.8	2.3	4.7	3.8	342.4	9.1	4.5	815.8	>1000
C2049	10.0	5.2	7.1	319.9	9.6	65.5	10.9	17.5	12.8	>1000	7.2
C2065	11.6	9.8	>1000	4.0	11.1	6.4	387.7	9.6	11.1	123.4	>1000
C2319	13.3	6.3	8.7	>1000	10.2	131.2	7.7	28.4	297.3	>1000	8.5
C2175	17.6	4.9	12.1	5.1	14.2	8.0	506.1	>1000	17.5	347.0	23.5
C2219	20.7	9.8	13.0	5.2	19.4	35.1	>1000	369.6	13.7	>1000	>1000
C2227	48.3	28.5	94.8	20.6	45.0	36.8	>1000	8.7	>1000	>1000	14.3
C2047	49.1	40.4	145.2	>1000	48.8	53.2	168.6	>1000	96.8	>1000	123.4
C2045	52.0	41.2	46.4	>1000	61.1	375.8	62.9	>1000	60.3	>1000	76.4
C2188	90.8	45.7	64.3	>1000	56.6	743.4	134.8	>1000	>1000	>1000	119.6
C2037	148.1	74.1	53.1	32.7	88.0	103.4	378.3	147.5	157.4	246.4	>1000
C2228	178.4	145.9	124.1	70.2	132.2	>1000	770.5	>1000	197.9	886.3	785.3
C2167	200.4	140.1	156.4	13.6	144.2	143.0	287.9	233.5	183.3	28.4	243.6
C2318	351.9	126.5	262.1	113.7	241.7	335.9	286.4	311.0	477.8	244.8	231.4
C2210	366.2	145.7	236.9	188.6	270.5	297.1	382.6	333.2	276.1	381.7	363.0
C2317	429.2	549.9	>1000	105.5	296.6	282.1	>1000	305.6	387.5	>1000	>1000
C2172	451.6	246.0	324.0	214.0	257.3	>1000	363.5	>1000	486.9	>1000	199.7
C2070	584.0	532.7	856.2	260.7	529.0	709.6	884.3	629.7	802.5	838.8	578.2
C2321	843.9	254.3	>1000	648.9	>1000	627.1	400.1	316.5	693.4	445.2	>1000

IC50 (ng/ml)

682

683 **Extended data Fig. 8: Breadth of anti-SARS-CoV-2 RBD antibodies elicited after prime and**

684 **boost vaccination**. **a-b**, IC$_{50}$ values for n=40 neutralizing antibodies isolated after prime **(a)** or

685 boost **(b)** against indicated mutant SARS-CoV-2 pseudoviruses. Color gradient indicates IC$_{50}$

686 values ranging from 0 (white) to 1000 ng/ml (red).

687

688

689

REFERENCES

1   Wang, Z. *et al.* Naturally enhanced neutralizing breadth against SARS-CoV-2 one year after infection. *Nature*, doi:10.1038/s41586-021-03696-9 (2021).

2   Goel, R. R. *et al.* Distinct antibody and memory B cell responses in SARS-CoV-2 naive and recovered individuals following mRNA vaccination. *Sci Immunol* **6**, doi:10.1126/sciimmunol.abi6950 (2021).

3   Robbiani, D. F. *et al.* Convergent antibody responses to SARS-CoV-2 in convalescent individuals. *Nature* **584**, 437-442, doi:10.1038/s41586-020-2456-9 (2020).

4   Apostolidis, S. A. *et al.* Altered cellular and humoral immune responses following SARS-CoV-2 mRNA vaccination in patients with multiple sclerosis on anti-CD20 therapy. *medRxiv*, 2021.2006.2023.21259389, doi:10.1101/2021.06.23.21259389 (2021).

5   Sokal, A. *et al.* Memory B cells control SARS-CoV-2 variants upon mRNA vaccination of naive and COVID-19 recovered individuals. *bioRxiv*, 2021.2006.2017.448459, doi:10.1101/2021.06.17.448459 (2021).

6   Turner, J. S. *et al.* SARS-CoV-2 mRNA vaccines induce persistent human germinal centre responses. *Nature*, doi:10.1038/s41586-021-03738-2 (2021).

7   Gaebler, C. *et al.* Evolution of antibody immunity to SARS-CoV-2. *Nature* **591**, 639-644, doi:10.1038/s41586-021-03207-w (2021).

8   Schmidt, F. *et al.* Measuring SARS-CoV-2 neutralizing antibody activity using pseudotyped and chimeric viruses. *J Exp Med* **217**, doi:10.1084/jem.20201181 (2020).

9   Pilishvili, T. *et al.* Interim Estimates of Vaccine Effectiveness of Pfizer-BioNTech and Moderna COVID-19 Vaccines Among Health Care Personnel - 33 U.S. Sites, January-March 2021. *MMWR Morb Mortal Wkly Rep* **70**, 753-758, doi:10.15585/mmwr.mm7020e2 (2021).

10   Lopez Bernal, J. *et al.* Effectiveness of Covid-19 Vaccines against the B.1.617.2 (Delta) Variant. *N Engl J Med*, doi:10.1056/NEJMoa2108891 (2021).

11   Reynolds, C. J. *et al.* Prior SARS-CoV-2 infection rescues B and T cell responses to variants after first vaccine dose. *Science*, doi:10.1126/science.abh1282 (2021).

12   Wang, Z. *et al.* mRNA vaccine-elicited antibodies to SARS-CoV-2 and circulating variants. *Nature* **592**, 616-622, doi:10.1038/s41586-021-03324-6 (2021).

13   Stamatatos, L. *et al.* mRNA vaccination boosts cross-variant neutralizing antibodies elicited by SARS-CoV-2 infection. *Science*, doi:10.1126/science.abg9175 (2021).

14   West, A. P. *et al.* Detection and characterization of the SARS-CoV-2 lineage B.1.526 in New York. *bioRxiv*, doi:10.1101/2021.02.14.431043 (2021).

15   Edara, V. V. *et al.* Infection and Vaccine-Induced Neutralizing-Antibody Responses to the SARS-CoV-2 B.1.617 Variants. *N Engl J Med*, doi:10.1056/NEJMc2107799 (2021).

16   Planas, D. *et al.* Reduced sensitivity of SARS-CoV-2 variant Delta to antibody neutralization. *Nature*, doi:10.1038/s41586-021-03777-9 (2021).

17   Victora, G. D. & Nussenzweig, M. C. Germinal centers. *Annu Rev Immunol* **30**, 429-457, doi:10.1146/annurev-immunol-020711-075032 (2012).

18   Brouwer, P. J. M. *et al.* Potent neutralizing antibodies from COVID-19 patients define multiple targets of vulnerability. *Science* **369**, 643-650, doi:10.1126/science.abc5902 (2020).

44

733   19   Kreer, C. *et al.* Longitudinal Isolation of Potent Near-Germline SARS-CoV-2-
734   Neutralizing Antibodies from COVID-19 Patients. *Cell* **182**, 843-854 e812,
735   doi:10.1016/j.cell.2020.06.044 (2020).
736   20   Seydoux, E. *et al.* Analysis of a SARS-CoV-2-Infected Individual Reveals Development
737   of Potent Neutralizing Antibodies with Limited Somatic Mutation. *Immunity* **53**, 98-105
738   e105, doi:10.1016/j.immuni.2020.06.001 (2020).
739   21   Taylor, J. J., Pape, K. A., Steach, H. R. & Jenkins, M. K. Humoral immunity. Apoptosis
740   and antigen affinity limit effector cell differentiation of a single naive B cell. *Science* **347**,
741   784-787, doi:10.1126/science.aaa1342 (2015).
742   22   Muecksch, F. *et al.* Development of potency, breadth and resilience to viral escape
743   mutations in SARS-CoV-2 neutralizing antibodies. *bioRxiv*,
744   doi:10.1101/2021.03.07.434227 (2021).
745   23   Amanna, I. J., Carlson, N. E. & Slifka, M. K. Duration of humoral immunity to common
746   viral and vaccine antigens. *N Engl J Med* **357**, 1903-1915, doi:10.1056/NEJMoa066092
747   (2007).
748   24   Davis, C. W. *et al.* Influenza vaccine-induced human bone marrow plasma cells decline
749   within a year after vaccination. *Science* **370**, 237-241, doi:10.1126/science.aaz8432
750   (2020).
751   25   Halliley, J. L. *et al.* Long-Lived Plasma Cells Are Contained within the CD19(-
752   )CD38(hi)CD138(+) Subset in Human Bone Marrow. *Immunity* **43**, 132-145,
753   doi:10.1016/j.immuni.2015.06.016 (2015).
754   26   Slifka, M. K., Antia, R., Whitmire, J. K. & Ahmed, R. Humoral immunity due to long-
755   lived plasma cells. *Immunity* **8**, 363-372, doi:10.1016/s1074-7613(00)80541-5 (1998).
756   27   Dan, J. M. *et al.* Immunological memory to SARS-CoV-2 assessed for up to 8 months
757   after infection. *Science* **371**, doi:10.1126/science.abf4063 (2021).
758   28   Sakharkar, M. *et al.* Prolonged evolution of the human B cell response to SARS-CoV-2
759   infection. *Sci Immunol* **6**, doi:10.1126/sciimmunol.abg6916 (2021).
760   29   Widge, A. T. *et al.* Durability of Responses after SARS-CoV-2 mRNA-1273
761   Vaccination. *N Engl J Med* **384**, 80-82, doi:10.1056/NEJMc2032195 (2021).
762   30   Wajnberg, A. *et al.* Robust neutralizing antibodies to SARS-CoV-2 infection persist for
763   months. *Science* **370**, 1227-1230, doi:10.1126/science.abd7728 (2020).
764   31   Pegu, A. *et al.* Durability of mRNA-1273-induced antibodies against SARS-CoV-2
765   variants. *bioRxiv*, doi:10.1101/2021.05.13.444010 (2021).
766   32   Chen, R. E. *et al.* Resistance of SARS-CoV-2 variants to neutralization by monoclonal
767   and serum-derived polyclonal antibodies. *Nat Med* **27**, 717-726, doi:10.1038/s41591-021-
768   01294-w (2021).
769   33   Abu-Raddad, L. J., Chemaitelly, H., Butt, A. A. & National Study Group for, C.-V.
770   Effectiveness of the BNT162b2 Covid-19 Vaccine against the B.1.1.7 and B.1.351
771   Variants. *N Engl J Med* **385**, 187-189, doi:10.1056/NEJMc2104974 (2021).
772   34   Hacisuleyman, E. *et al.* Vaccine Breakthrough Infections with SARS-CoV-2 Variants. *N
773   Engl J Med* **384**, 2212-2218, doi:10.1056/NEJMoa2105000 (2021).
774   35   Lumley, S. F. *et al.* Antibody Status and Incidence of SARS-CoV-2 Infection in Health
775   Care Workers. *N Engl J Med* **384**, 533-540, doi:10.1056/NEJMoa2034545 (2021).
776   36   McHeyzer-Williams, L. J., Milpied, P. J., Okitsu, S. L. & McHeyzer-Williams, M. G.
777   Class-switched memory B cells remodel BCRs within secondary germinal centers. *Nat
778   Immunol* **16**, 296-305, doi:10.1038/ni.3095 (2015).

779 37 Mesin, L. *et al.* Restricted Clonality and Limited Germinal Center Reentry Characterize
780   Memory B Cell Reactivation by Boosting. *Cell* **180**, 92-106 e111,
781   doi:10.1016/j.cell.2019.11.032 (2020).
782 38 Pape, K. A., Taylor, J. J., Maul, R. W., Gearhart, P. J. & Jenkins, M. K. Different B cell
783   populations mediate early and late memory during an endogenous immune response.
784   *Science* **331**, 1203-1207, doi:10.1126/science.1201730 (2011).
785 39 Viant, C. *et al.* Antibody Affinity Shapes the Choice between Memory and Germinal
786   Center B Cell Fates. *Cell* **183**, 1298-1311 e1211, doi:10.1016/j.cell.2020.09.063 (2020).
787 40 Sokal, A. *et al.* Maturation and persistence of the anti-SARS-CoV-2 memory B cell
788   response. *Cell* **184**, 1201-1213 e1214, doi:10.1016/j.cell.2021.01.050 (2021).
789 41 Feng, L. *et al.* An adenovirus-vectored COVID-19 vaccine confers protection from
790   SARS-COV-2 challenge in rhesus macaques. *Nat Commun* **11**, 4207,
791   doi:10.1038/s41467-020-18077-5 (2020).
792 42 Hassan, A. O. *et al.* A Single-Dose Intranasal ChAd Vaccine Protects Upper and Lower
793   Respiratory Tracts against SARS-CoV-2. *Cell* **183**, 169-184 e113,
794   doi:10.1016/j.cell.2020.08.026 (2020).
795 43 Greaney, A. J. *et al.* Antibodies elicited by mRNA-1273 vaccination bind more broadly
796   to the receptor binding domain than do those from SARS-CoV-2 infection. *Sci Transl*
797   *Med* **13**, doi:10.1126/scitranslmed.abi9915 (2021).
798 44 Pardi, N. *et al.* Expression kinetics of nucleoside-modified mRNA delivered in lipid
799   nanoparticles to mice by various routes. *J Control Release* **217**, 345-351,
800   doi:10.1016/j.jconrel.2015.08.007 (2015).
801 45 Wu, K. *et al.* Preliminary Analysis of Safety and Immunogenicity of a SARS-CoV-2
802   Variant Vaccine Booster. *medRxiv*, 2021.2005.2005.21256716,
803   doi:10.1101/2021.05.05.21256716 (2021).
804 46 Khoury, D. S. *et al.* Neutralizing antibody levels are highly predictive of immune
805   protection from symptomatic SARS-CoV-2 infection. *Nat Med* **27**, 1205-1211,
806   doi:10.1038/s41591-021-01377-8 (2021).
807 47 Wu, F. *et al.* A new coronavirus associated with human respiratory disease in China.
808   *Nature* **579**, 265-269, doi:10.1038/s41586-020-2008-3 (2020).
809 48 Amanat, F. *et al.* A serological assay to detect SARS-CoV-2 seroconversion in humans.
810   *Nat Med* **26**, 1033-1036, doi:10.1038/s41591-020-0913-5 (2020).
811 49 Grifoni, A. *et al.* Targets of T Cell Responses to SARS-CoV-2 Coronavirus in Humans
812   with COVID-19 Disease and Unexposed Individuals. *Cell* **181**, 1489-1501 e1415,
813   doi:10.1016/j.cell.2020.05.015 (2020).
814 50 Barnes, C. O. *et al.* Structures of Human Antibodies Bound to SARS-CoV-2 Spike
815   Reveal Common Epitopes and Recurrent Features of Antibodies. *Cell* **182**, 828-842 e816,
816   doi:10.1016/j.cell.2020.06.025 (2020).
817 51 Weisblum, Y. *et al.* Escape from neutralizing antibodies by SARS-CoV-2 spike protein
818   variants. *Elife* **9**, doi:10.7554/eLife.61312 (2020).
819 52 Wang, Z. *et al.* Enhanced SARS-CoV-2 neutralization by dimeric IgA. *Sci Transl Med*
820   **13**, doi:10.1126/scitranslmed.abf1555 (2021).
821 53 Gupta, N. T. *et al.* Change-O: a toolkit for analyzing large-scale B cell immunoglobulin
822   repertoire sequencing data. *Bioinformatics* **31**, 3356-3358,
823   doi:10.1093/bioinformatics/btv359 (2015).

824   54   Soto, C. *et al.* High frequency of shared clonotypes in human B cell receptor repertoires.
825   *Nature* **566**, 398-402, doi:10.1038/s41586-019-0934-8 (2019).
826   55   Guo, Y., Chen, K., Kwong, P. D., Shapiro, L. & Sheng, Z. cAb-Rep: A Database of
827   Curated Antibody Repertoires for Exploring Antibody Diversity and Predicting Antibody
828   Prevalence. *Front Immunol* **10**, 2365, doi:10.3389/fimmu.2019.02365 (2019).
829